Quasiclassical magnetotransport in a random array of antidots

D. G. Polyakov,[1,*] F. Evers,[1] A. D. Mirlin,[1,2,†] and P. Wölfle[1,2]
[1]*Institut für Nanotechnologie, Forschungszentrum Karlsruhe, D-76021 Karlsruhe, Germany*
[2]*Institut für Theorie der Kondensierten Materie, Universität Karlsruhe, D-76128 Karlsruhe, Germany*
(Received 24 April 2001; published 23 October 2001)

We study theoretically the magnetoresistance $\rho_{xx}(B)$ of a two-dimensional electron gas scattered by a random ensemble of impenetrable discs in the presence of a long-range correlated random potential. We believe that this model describes a high-mobility semiconductor heterostructure with a random array of antidots. We show that the interplay of scattering by the two types of disorder generates new behavior of $\rho_{xx}(B)$ which is absent for only one kind of disorder. We demonstrate that even a weak long-range disorder becomes important with increasing B. In particular, although $\rho_{xx}(B)$ vanishes in the limit of large B when only one type of disorder is present, we show that it keeps growing with increasing B in the antidot array in the presence of smooth disorder. The reversal of the behavior of $\rho_{xx}(B)$ is due to a mutual destruction of the quasiclassical localization induced by a strong magnetic field: specifically, the adiabatic localization in the long-range Gaussian disorder is washed out by the scattering on hard discs, whereas the adiabatic drift and related percolation of cyclotron orbits destroys the localization in the dilute system of hard discs. For intermediate magnetic fields in a dilute antidot array, we show the existence of a strong negative magnetoresistance, which leads to a nonmonotonic dependence of $\rho_{xx}(B)$.

DOI: 10.1103/PhysRevB.64.205306 PACS number(s): 73.43.Qt, 73.63.Kv

I. INTRODUCTION

In recent years, there has been a revival of interest in *quasiclassical* transport properties of a two-dimensional electron gas (2DEG). This has been largely motivated by the experimental progress in controlled preparation of nanostructured semiconductor systems[1] and, in particular, by the experimental and practical importance of high-mobility heterostructures, in which impurities are separated from the 2DEG by a wide spacer. On the theoretical side, much of the recent interest in quasiclassics on the nanometer scale has been related to the realization that the classical dynamics in a disordered system is in fact much richer than the idealized Drude picture suggests. Indeed, as far as ballistic mesoscopic systems are concerned, electron transport has been studied in terms of quasiclassical dynamics in great detail.[2] However, in diffusive systems with smooth disorder, a quasiclassical treatment of electron kinetics is also appropriate and has been shown to lead to different transport regimes. To describe the transport properties of such system, one sometimes has to completely abandon theories based on the Boltzmann equation. In Boltzmann transport theory, formulated in terms of a set of relaxation times, quasiclassics leads to the Drude results: analytical behavior of the ac conductivity $\sigma(\omega)$ at $\omega \to 0$, zero magnetoresistance (MR), etc. It has been demonstrated, however, that quasiclassical *memory effects*, neglected in the conventional Boltzmann approach, yield a wealth of anomalous transport properties of a 2DEG subject to *long-range* disorder. In particular, non-Markovian kinetics gives rise to a quasiclassical zero-frequency anomaly (see Ref. 3 and references therein) in the ac response of a disordered 2DEG, associated with return processes in the presence of smooth inhomogeneities. Specifically, the return-induced correction to $\mathrm{Re}\,\sigma(\omega)$ exhibits a kink $\propto|\omega|$. Another manifestation of non-Markovian kinetics is a strong positive MR in low magnetic fields,[4] which is able to explain[5] the otherwise puzzling positive MR observed near half filling of the lowest Landau level in the fractional quantum Hall regime. The strength of the above anomalies depends on the ratio d/l, where d is the correlation radius of disorder, l the mean free path, and grows with increasing d/l as a power of this parameter. Since quantum corrections are governed by a different small parameter $1/k_F l \ll 1$, where k_F is the Fermi wave vector, it is the long-range correlations of disorder with $k_F d \gg 1$ that reveal the quasiclassical anomalies. The condition $k_F d \gg 1$ is typically well satisfied in high-mobility semiconductor heterostructures.

In this paper, we consider the quasiclassical magnetotransport properties of a 2DEG in a random array of antidots (AD). The transport (dc and far-infrared) properties of AD arrays, both periodic and random, have been the subject of many recent experiments, see, e.g., Refs. 6–12 and references therein. In periodic arrays (for a review see Refs. 13 and 14), interest has been focused on geometric resonances which are associated with the periodicity and result, in particular, in commensurability peaks in the MR.[15–18] On the other hand, random arrays (see, e.g., Refs. 19,20,12,9,7 and 6) constitute a remarkable disordered system where the AD's play the role of hard-wall scatterers. We aim to study the MR in random AD arrays and therefore assume that there exist two types of disorder: AD's, which we model as impenetrable hard discs that scatter electrons, and a smooth random potential, created in the heterostructures by charged impurities behind a spacer. The quasiclassical MR in each of the limits, where only one type of disorder is present, is well understood by now (see Sec. II). The purpose of the paper is to demonstrate that the interplay of the two types of disorder yields interesting physics that is absent in the limiting cases. We will show that, although in the extreme of a strong magnetic field $B \to \infty$ the dissipative resistivity $\rho_{xx}(B)$ *tends to zero* in either of the limiting cases, it *diverges* in the presence of both types of disorder. In particular, in the experimentally relevant situation of relatively weak long-range disorder, i.e.,

when the mean free path at zero B is determined by scattering on AD's, the presence of the weak long-range fluctuations will nonetheless become of crucial importance with increasing B. It is worth noting that our model can also be applicable to the description of the MR in an unstructured 2DEG with residual interface impurities playing the role of antidots (large-angle scattering on residual impurities is known to become important in unstructured samples with a wide spacer).[21–23]

The paper is organized as follows. We give a brief review of past work on the quasiclassical MR in Sec. II. In the body of the paper, we first consider in Sec. III the MR at a moderately strong B, when the collision time for scattering on AD's is not affected by the magnetic field. Then, in Sec. IV, we turn to the limit of strong B, where the collision time is renormalized as compared to the Drude value and, in the extreme of very large B, a single act of scattering involves ''skipping'' of cyclotron orbits along the surface of AD's. The whole picture turns out to be rather complex and we choose the following logic of presentation. We fix the zero-B mean free paths for scattering on AD's and on the long-range disorder and for different values of the density n of AD's sweep the magnetic field. In Sec. III we start with the ''hydrodynamic limit'' of infinite n and then gradually decrease n. In Sec. IV we first consider a single act of scattering on an AD for large B, then proceed to analyze the strong-B transport in an AD array. We present results of numerical simulations in Sec. V and summarize in Sec. VI [where the qualitative behavior of $\rho_{xx}(B)$ is illustrated in Fig. 13].

II. OUTLINE OF KNOWN RESULTS: LIMITING CASES

A. Lorentz model

We start by briefly recalling the known results for the classical Lorentz model in two dimensions (hard discs of radius a, randomly placed with a concentration n; we assume that $na^2 \ll 1$ and $k_F a \gg 1$, so that the mean free path $l_S = 3/8na$). This is a good model for an AD array in a heterostructure. As was pointed out in Refs. 24 and 25, Drude theory fails completely to describe magnetotransport in this system. In the limit $n \to \infty$, $a \to 0$, with l_S held fixed, the resistivity depends on a single variable l_S/R_c, where R_c is the Larmor radius, and reads,[25] in units of the zero-B resistivity ρ_0,

$$\frac{\rho_{xx}(B)}{\rho_0} = F\left(\frac{l_S}{R_c}\right), \tag{1}$$

with $F(0)=1$ and $F(x \gg 1) \simeq 9\pi/8x \ll 1$. In Drude theory, the dissipative resistivity is not affected by a magnetic field and $F(x)=1$ for all x. The nontrivial kinetic problem (1) is in fact fully solvable and the exact expression for the conductivity tensor at arbitrary l_S/R_c can be found in Refs. 25 and 26 (see also Refs. 26 and 27 for numerical simulations of the problem).

The falloff of $\rho_{xx} \propto B^{-1}$ is related to the peculiarity of the Lorentz model: at finite B, there are electrons that move freely in steady cyclotron orbits and never hit a scatterer; those electrons do not contribute to ρ_{xx} and their density grows with increasing B. The conductivity is then due to electrons that experience multiple collisions with a scatterer by moving in ''rosette'' orbits around it (Fig. 1) until they hit another scatterer, which results in a diffusive hopping of the ''rosette states.'' At finite concentration n, the Lorentz model has a metal-insulator transition[24,25] at $R_c \sim n^{-1/2}$: for larger B the dissipative conductivity is strictly zero, as shown in Fig. 1.

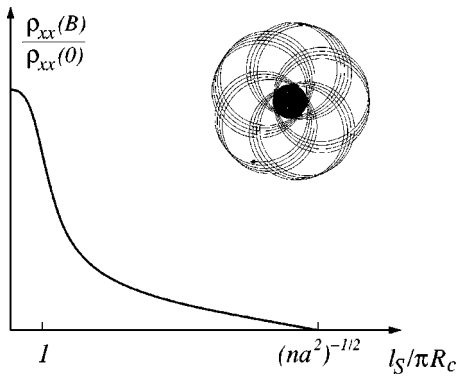

FIG. 1. Schematic behavior of the magnetoresistivity $\rho_{xx}(B)$ as a function of $l_S/\pi R_c$ in the Lorentz model. Inset: Rosette orbit of an electron bound to a hard disc (shown by the shaded circle) in a magnetic field.

B. Long-range disorder

Now let us recall what is known about MR in the case of a smooth (allowing for a quasiclassical treatment) Gaussian (in the sense of statistics of fluctuations) random scalar potential. There are two sources of quasiclassical MR (we consider elastic scattering on an isotropic Fermi surface).

First, note that the MR is strictly zero in Boltzmann theory only in the limit of white-noise disorder, whereas if disorder is correlated on a finite spatial scale d, the collision-integral approximation allows for a finite MR,[28,29] due to a cyclotron bending of trajectories within this correlation radius. This simple effect is governed by the parameter d/R_c [at small B it yields $\Delta\rho_{xx}/\rho_0 \sim -(d/R_c)^2$].

Second, there is[4] MR associated with memory effects and, to calculate this, one has to go beyond the collision-integral approximation. The memory effects are brought about by correlations of scattering acts at the points where quasiclassical trajectories self-intersect. These effects give the main contribution to $\Delta\rho_{xx}/\rho_0$ at large enough B, where the governing parameter is d/δ with δ being a characteristic shift of the center of a cyclotron orbit after one revolution. For $R_c/d \gtrsim 1$ the shift is (see Ref. 30 and references therein)

$$\delta \sim R_c(R_c/l_L)^{1/2}, \quad R_c \gtrsim d, \tag{2}$$

where l_L is the mean free path in the smooth random potential (experimentally, $l_L/d \sim 10^2$–10^3 in high-mobility samples). According to Ref. 4, $\Delta\rho_{xx}/\rho_0 \sim (d/\delta)^3 \lesssim 1$. The return-induced contribution becomes much larger than that related to the effect of B on the collision integral at

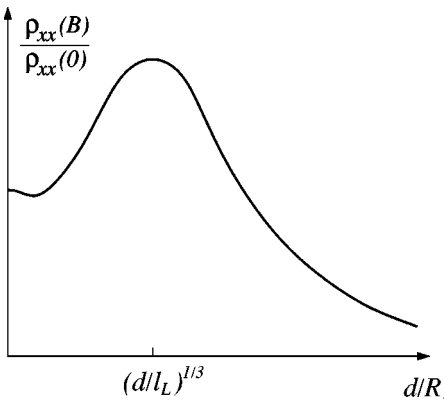

FIG. 2. Schematic behavior of the magnetoresistivity $\rho_{xx}(B)$ as a function of d/R_c for a Gaussian smooth random potential.

$(\delta/R_c)^2 \ll d/\delta$, i.e., at $R_c \ll l_L(d/l_L)^{2/5}$. The exact expression for the MR in the limit $(\delta/R_c)^2 \ll d/\delta \ll 1$ in a heterostructure with a spacer d is[4]

$$\frac{\Delta\rho_{xx}(B)}{\rho_0} = \frac{2\zeta(3/2)}{\pi}\left(\frac{d}{l_L}\right)^3\left(\frac{l_L}{R_c}\right)^{9/2}. \tag{3}$$

This equation is valid with increasing magnetic field up to $d/\delta \sim 1$, where $\Delta\rho_{xx}(B)/\rho_0$ becomes of order unity. At higher fields, when $\delta/d \ll 1$, the strong positive MR is followed by a sharp (exponential) falloff of ρ_{xx} with growing B:[30]

$$\ln\left(\frac{\rho_{xx}}{\rho_0}\right) \sim -\left(\frac{d}{\delta}\right)^{2/3}, \tag{4}$$

which is due to the increasing adiabaticity of the electron dynamics and the related quasiclassical localization.[30,5] The self-intersection induced MR, given by Eq. (3), may be considered as a precursor of the adiabatic localization. In the limit of large B, when R_c/d becomes small, δ is given by

$$\delta \sim R_c^2/(dl_L)^{1/2}, \quad R_c \lesssim d. \tag{5}$$

The nonmonotonic behavior (3) and (4) of the MR in the case of a purely Gaussian long-range random potential is illustrated in Fig. 2.

To conclude the brief overview, it is worth noting that in the limit of weak inhomogeneities the return-induced MR depends in an essential way on the behavior of the disorder under time reversal. In particular, it is strongly enhanced in the case of a random magnetic field.[4]

III. EFFECT OF CYCLOTRON DRIFT ON TRANSPORT IN ANTIDOT ARRAYS

A. Parameters of the problem

We now turn to the MR in the presence of both a random array of hard discs and long-range Gaussian disorder, which we characterize by the mean free paths at zero magnetic field l_S and l_L, respectively. We assume that $l_S/l_L \ll 1$, which describes a typical experimental situation. As in Sec. II, n will denote the concentration of AD's, a their radius, d the correlation length of the smooth random potential, R_c the cyclotron radius, and δ the characteristic shift, due to scattering on the long-range disorder, of the cyclotron orbit after one revolution. Throughout the paper we assume $d/a \gg 1$.

We are interested in strong effects in the behavior of $\rho_{xx}(B)$: for $l_S/l_L \ll 1$, these can only occur if $R_c/l_S \lesssim 1$. Moreover, for the most part of the paper (namely, with the exception of Sec. IV A), we consider magnetic fields which are sufficiently strong in the sense that $\delta/d \lesssim 1$. In this case, the motion of electrons is characterized by rapid cyclotron rotation around the guiding center and slow drift of the latter along equipotential lines of a smooth random potential. Most of these lines are closed, which leads to localization of particles trapped on them. The effect of scattering by AD's is to induce transitions between equipotential contours and, in this way, allow the localized particles to escape.

B. Hydrodynamic limit

Let us first consider the "hydrodynamic limit" ($n \to \infty$, $a \to 0$, $l_S = \text{const}$). Clearly, in this limit, the effects yielding the falloff of $\rho_{xx} \propto B^{-1}$ [Eq. (1)] are washed out by infinitesimally weak long-range disorder. One might think that then the Drude formula works and $\rho_{xx}(B)/\rho_0 \simeq 1$ for all B. In fact, however, this is not true and even a small ($l_S/l_L \ll 1$) amount of smooth disorder becomes a relevant perturbation with increasing B. Indeed, in the limit of large B (namely, for $\delta/d \ll 1$), the problem can be mapped onto that of advection-diffusion transport,[31] i.e., of a Brownian motion with a diffusion coefficient D_0 in a spatially random velocity field $\mathbf{v}(\mathbf{r})$ ("steady flow") with $\nabla \cdot \mathbf{v} = 0$ ("incompressible fluid"). In this mapping, the field $\mathbf{v}(\mathbf{r})$ describes the adiabatic drift of guiding centers of cyclotron orbits due to long-range inhomogeneities and $D_0 \sim R_c^2/\tau_S$, where τ_S is the momentum relaxation time for scattering on AD's. The result for the effective (macroscopic) diffusion coefficient D in the advection-diffusion problem[31] is

$$D \sim D_0(v_d d/D_0)^{10/13} \tag{6}$$

if $v_d d \gtrsim D_0$ and $D = D_0$ otherwise. Here v_d is a characteristic amplitude of the fluctuations of $\mathbf{v}(\mathbf{r})$ [see Eqs. (11) and (12) below]. Hence the conductivity will be strongly enhanced by even a weak long-range disorder provided $v_d d/D_0 \gg 1$. Since this parameter is a growing function of B, the effect of smooth disorder is amplified by the magnetic field. The reason is percolation of cyclotron orbits through long-range inhomogeneities: the percolation-dominated D can be written as a product $v_d w$, where $w \ll d$ is a characteristic width of links of the percolation network. The equation $w \sim d(D_0/v_d d)^{3/13}$ in the advection-diffusion problem comes from the condition of connectivity of the network $w^2 v_d/L(w) \sim D_0$, where

$$L(w) \sim d(d/w)^{7/3} \tag{7}$$

is a typical length of the network link.[31] Note that the size $\xi(w)$ of the elementary cell of the percolation network [i.e., a characteristic end-to-end distance for the link of length $L(w)$] scales as[31]

$$\xi(w) \sim d(d/w)^{4/3}. \tag{8}$$

Although the advection-diffusion model has become popular for the description of transport in the high-B limit (in particular, in the quantum Hall regime[32,33]) we should be careful to check if the scattering on AD's can actually be described in this model in terms of the diffusion coefficient D_0. Clearly, this requires that w be larger than a hopping length for the diffusion process, which means $w \gg R_c$. While this condition is satisfied in the extreme of large B, a nontrivial transport regime may occur with increasing B in which $D \gg D_0$ but $w \ll R_c$ (as we will see below, this is the case if the long-range disorder is not too weak). In this regime, the main contribution to D comes from electrons that move freely along the critical links: the "ballistic" motion along the percolating path is contrasted with the transverse (across the drift trajectory) diffusion in the advection-diffusion regime. In other words, the number of collisions with AD's during the drift along a critical link of the percolation network is now of order unity. As in the advection-diffusion regime, the number of passages of the network link between two consecutive changes of critical cells is also of order unity. It follows that w obeys the simple scaling $L(w) \sim v_d \tau_S$, so that the result for $D \sim v_d w$ is

$$D \sim v_d d (d/v_d \tau_S)^{3/7}, \tag{9}$$

which should be compared, as in the advection-diffusion problem, with D_0: Eq. (9) is valid when $D \gtrsim D_0$. Note that in this new regime D does not contain the hopping length, which may be even larger than d.

We are now prepared to calculate the MR. The chaotic scattering on the long-range potential crosses over into the adiabatic drift with increasing B at R_c of order

$$\tilde{R}_c = d (l_L/d)^{1/3}, \tag{10}$$

where δ/d becomes of order unity [cf. Eqs. (3) and (4)]. At this field, the MR is still weak and transport is completely determined by scattering on AD's, whereas at larger B we can already use the high-field formulas (6) and (9) and write $\rho_{xx}(B)/\rho_0 \simeq D/D_0$. The characteristic drift velocity v_d that should be substituted into Eqs. (6) and (9) reads (see, e.g., Ref. 30):

$$v_d = v_F \frac{R_c}{(d l_L)^{1/2}} s\left(\frac{d}{R_c}\right), \tag{11}$$

where v_F is the Fermi velocity and the function $s(x)$ is given by

$$s(x) \sim \begin{cases} x^{1/2}, & x \ll 1 \\ 1, & x \gg 1. \end{cases} \tag{12}$$

Which of Eqs. (6) and (9) should be used depends on the ratio w/R_c, as explained above. Remarkably, the ratio D/D_0 for both Eqs. (6) and (9) depends only on two variables, $x = d/R_c$ and $v_d \tau_S/d = p x^{-1} s(x)$, where

$$p = \frac{l_S}{\sqrt{d l_L}}. \tag{13}$$

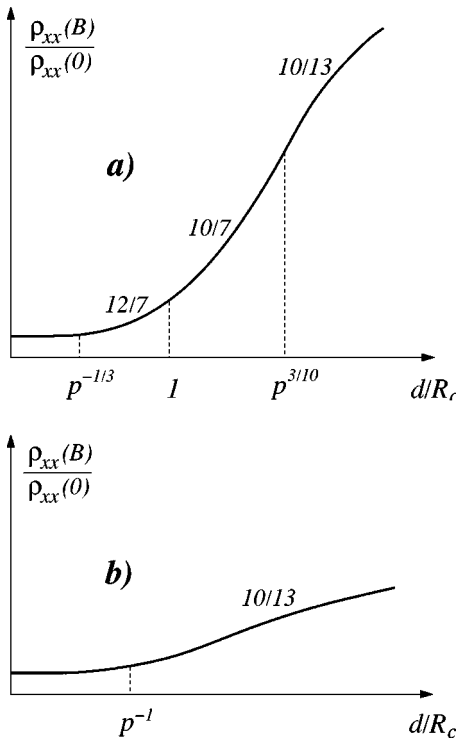

FIG. 3. Schematic behavior of the magnetoresistivity $\rho_{xx}(B)$ as a function of d/R_c in the hydrodynamic limit $n \to \infty$, $a \to 0$, l_S = const for (a) $p = l_S/\sqrt{d l_L} \gg 1$ and (b) $p \ll 1$. The numbers denote the exponent of the power-law dependence of $\rho_{xx}(B)$.

As a result, the behavior of the MR as a function of B depends, at $a \to 0$, on the single parameter p, so that we can write

$$\frac{\rho_{xx}(B)}{\rho_0} = f\left(\frac{d}{R_c}, p\right). \tag{14}$$

Notice that even though we consider the case $l_S/l_L \ll 1$, the parameter p may be large since the long-range disorder is weak, i.e., $d/l_L \ll 1$.

At $p \gg 1$, the MR remains small, i.e., $f(x,p) \simeq 1$, for all $x \ll p^{-1/3}$. On the upper boundary of this interval, the percolation starts to renormalize D in accordance with Eq. (9), which yields a power-law growth of $\rho_{xx}(B)$ with further increasing B:

$$f(x,p) \sim (p x^3)^{4/7}, \quad p^{-1/3} \ll x \ll 1; \tag{15}$$

$$(p x^{5/2})^{4/7}, \quad 1 \ll x \ll p^{3/10}. \tag{16}$$

The scaling behavior changes between Eqs. (15) and (16) at $x \sim 1$ because of the change in the dependence of v_d on B at $R_c/d \sim 1$. At still larger B, D obeys Eq. (6), which gives

$$f(x,p) \sim (px)^{10/13}, \quad p^{3/10} \ll x. \tag{17}$$

Equations (15)–(17) are illustrated in Fig. 3(a).

At $p \ll 1$, the range of x where the enhancement of the conductivity is described by Eq. (9) shrinks away, so that $f(x,p) \simeq 1$ for all $x \ll p^{-1}$ and behaves according to Eq. (17) at larger x [see Fig. 3(b)]. This establishes the meaning of the parameter p: if $p \ll 1$, the Drude regime does not match with

increasing B the advection-diffusion regime (6) directly, but through the intermediate ''one-hop'' regime (9), whereas if p is large, this intermediate phase is absent. Equation (17) tells us that $\rho_{xx}(B) \propto B^{10/13}$ at $B \to \infty$. The divergence takes place whatever the ratio l_S/l_L, even if the long-range disorder is weak and does not play a role at $B=0$. This behavior differs drastically from that given by either of Eqs. (1) and (4).

C. Finite density of antidots

So far, in Eqs. (14)–(17), the scattering on AD's has been characterized by l_S only, through the single parameter p [Eq. (13)], which implies the hydrodynamic limit $n \to \infty$, $a \to 0$. Now we take into account finite-n effects. We begin as before with the case of large p. Additional relevant dimensionless parameters appear, in particular, $nR_c d$. Also, since for a fixed l_S decreasing n means increasing a, the parameter δ/a may become relevant, in which case the scattering on AD's will be affected by the magnetic field in an essential way and the collision time will not be given by τ_S. We will consider effects governed by the parameter δ/a in Sec. IV. Until then, let us assume that δ/a is sufficiently large, so that this parameter plays no role for typical electron trajectories.

Clearly, if $\delta/a \gg 1$, stable rosette states[24,25] are still destroyed by the scattering on the long-range potential. Naively, one could think that scattering on AD's is then chaotic (no trace of the rosette-state dynamics) and Eqs. (14)–(17) apply. In actual fact, provided $nR_c d \ll 1$, multiple collisions with the same AD do occur even for $\delta/a \gg 1$, as we will see below. At large p, the former condition is satisfied with increasing B before δ/a gets small. Multiple returns in a dense AD array become possible because of the adiabatic localization, which develops at $\delta/d \lesssim 1$.

Let us start by considering the drift regime under the condition $nR_c d \ll 1$, $R_c/d \gg 1$. Typical trajectories of guiding centers are closed loops of size $\sim d$, which means that trajectories of electrons circling along cyclotron orbits are bound to within thin rings of width $\sim d$ and radius R_c. The area of a strip between the inner and outer radii of the rings is $\sim R_c d$ and, if $nR_c d \ll 1$, in most rings there are no AD's. Electrons in these rings are adiabatically localized and do not, in the adiabatic approximation, contribute to $\rho_{xx}(B)$ (we will consider the possibility of nonadiabatic decay of these states in Sec. III E). There are, however, rare rings with a single AD. For electrons in these rings, a typical time $\tilde{\tau}_S$ between collisions with AD's is much shorter than τ_S. Indeed, the number of cyclotron revolutions before returning to the region of size δ around the AD is typically d/δ, while the probability of hitting the AD during one such sweep is $\sim a/\delta$. It follows that the number of cyclotron revolutions before the electron hits the AD is $\sim d/a$, i.e.,

$$\tilde{\tau}_S \sim R_c d/v_F a, \tag{18}$$

which gives $\tilde{\tau}_S/\tau_S \sim nR_c d \ll 1$.

Now, a single collision with an AD does not lead to a breakaway from the AD. In fact, the electron experiences multiple collisions with a single AD and each time the center of the ring in which the electron is circling hops a distance $\sim R_c$: one can visualize this process as a random hopping of the center of the ring on a circle of radius R_c around the AD (see Fig. 4). The electron ''sticks'' to the AD for a time much longer than $\tilde{\tau}_S$. This somewhat intricate dynamics of ''hopping rings'' reminds one of the evolution of the rosette states:[24,25] in effect it is the adiabatic localization in the long-range potential that preserves the character of the rosette-state dynamics. A breakup will eventually happen when the electron picks up a very rare ring containing two AD's (the existence of such rings in the area $R_c \times R_c$ implies that $nR_c^2 \gg 1$, which we assume in this derivation). It is straightforward to check that the number of scatterings on a given AD before getting to another one is $\sim 1/nR_c d \gg 1$. Multiplying the latter by $\tilde{\tau}_S$, we find that the time it takes the electron to change AD's (separated by a distance $\sim R_c$) is $\sim \tau_S$, which yields the diffusion coefficient of electrons participating in this type of transport $\sim D_0$, the same as in Drude theory. These electrons, however, represent a small fraction of the total number of electrons, namely $\sim nR_c d$. Hence the contribution to the macroscopic diffusion coefficient from drift orbits of a characteristic size d is $\sim D_0 nR_c d \ll D_0$.

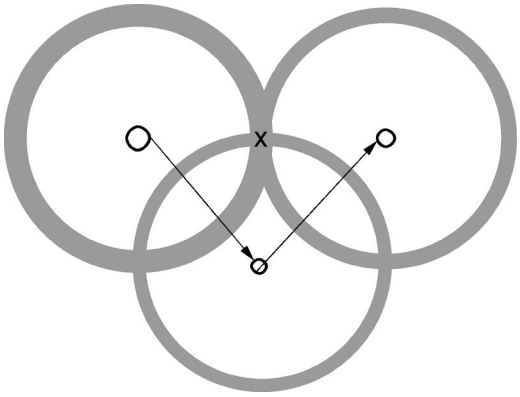

FIG. 4. A cartoon picture of scattering of a cyclotron orbit on an antidot at $a \ll \delta \ll d \ll R_c \ll (nd)^{-1}$. The position of the antidot is shown by a cross at the intersection of the rings (radius R_c, characteristic width d) which represent the area ''covered'' by the drifting cyclotron orbit. The arrows denote hopping of the guiding center of the orbit between drift trajectories shown by small loops. Provided $nR_c^2 \gg 1$, the particle will typically break away from the antidot when it picks up a ring containing one more antidot and hits the latter.

Having obtained the contribution of typical trajectories of size d, we should take into account that upon hitting an AD the particle may hop onto a drift trajectory of size ξ larger than d. To put it another way, although most trajectories with ξ in the interval $d \ll \xi \ll (nR_c)^{-1}$ are adiabatically localized, some of them hit AD's and mix with the short-scale trajectories of size d considered above. This mixing increases the total fraction of delocalized trajectories. To calculate the latter, note that the probability density $P(\xi)$ for a point to belong to a drift trajectory of size $\xi \gtrsim d$ (we define ξ as a characteristic radius of the area to within which the trajectory is bounded) scales as

$$P(\xi) \sim d/\xi^2. \tag{19}$$

No critical exponents are involved here. One way to get a quick proof of this is to realize that, according to percolation theory, for zero altitude on a relief map of a random landscape, the number of contours of radius ξ in the area $\xi\times\xi$ is of order unity. It follows that the (integrated over the altitude) fraction of space occupied by contours of size $\sim\xi$ is $\sim Lw/\xi^2\sim d/\xi$, where we used Eqs. (7) and (8), which yields Eq. (19). Thus the fraction of trajectories that are delocalized due to collisions with AD's is evaluated by integration

$$\int_d^{R_c} d\xi\, P(\xi)\min\{nR_c\xi,1\}\sim nR_c d\,\ln(1/nR_c d), \qquad (20)$$

which gives merely an additional logarithmic factor. One sees that the characteristic $\xi\lesssim(nR_c)^{-1}$ are within the limits of applicability of the derivation $\xi\ll R_c$ (trajectories with larger ξ give rise to a percolative contribution to ρ_{xx} considered in Sec. III B). Notice that drift trajectories that do not hit AD's may be infinitely extended only with zero measure and thus do not contribute to D. Accordingly, D is evaluated as a diffusion coefficient of electrons delocalized by the scattering on AD's. Since the relevant $\xi\ll R_c$, the characteristic hopping length associated with the change of AD's by these electrons is R_c. The characteristic rate of hopping between two different AD's is given by $n\langle\partial S/\partial t\rangle$, where $\langle\partial S/\partial t\rangle\sim\int d\xi\, P(\xi)[A(\xi)/\tilde{\tau}_S(\xi)]$ is the average rate at which the area explored by the particle stuck to an AD grows in time. Here

$$\tilde{\tau}_S(\xi)\sim\tilde{\tau}_S(d)\xi/d \qquad (21)$$

[with $\tilde{\tau}_S(d)$ defined in Eq. (18)] is the time the particle resides on a trajectory of size ξ before being scattered out by the same AD, and $A(\xi)\sim R_c\xi$ is the area probed during this time. These expressions for $\tilde{\tau}_S(\xi)$ and $A(\xi)$ are valid for $\xi\ll d(\delta/a)^{4/3}$, whereas at larger ξ the particle is scattered out before it comes full circle around the closed trajectory and both quantities do not depend on ξ. We see that $A(\xi)/\tilde{\tau}_S(\xi)$ does not depend on ξ and thus $\langle\partial S/\partial t\rangle\sim v_F a$ is determined by $\xi\sim d$. It follows that the hopping rate does not change with the inclusion of long trajectories and is given by τ_S^{-1}. Accordingly, the diffusion coefficient of delocalized particles is $\sim D_0$. We finally get for the macroscopic diffusion coefficient $D\sim D_0 nR_c d\,\ln(1/nR_c d)$, or, for the MR:

$$\frac{\rho_{xx}(B)}{\rho_0}\sim nR_c d\,\ln\frac{1}{nR_c d}. \qquad (22)$$

We thus see that, despite $\delta/a\gg1$, the resistivity is strongly suppressed as compared to the Drude result at $nR_c d\ll1$. We will return to this regime in Sec. IV E, where we will show that the actual condition for Eq. (22) to be valid is $\delta/a\gg(nR_c d)^{-3/4}$, whereas at smaller δ/a, $1\ll\delta/a\ll(nR_c d)^{-3/4}$, a slight modification, namely in the logarithmic factor in Eq. (22), is necessary.

The falloff of the MR described by Eq. (22) is illustrated in Fig. 5(a). Shown here is also the percolative growth of $\rho_{xx}(B)$ into which the falloff crosses over at sufficiently large B. As is clear from Fig. 5(a), in the above derivation we

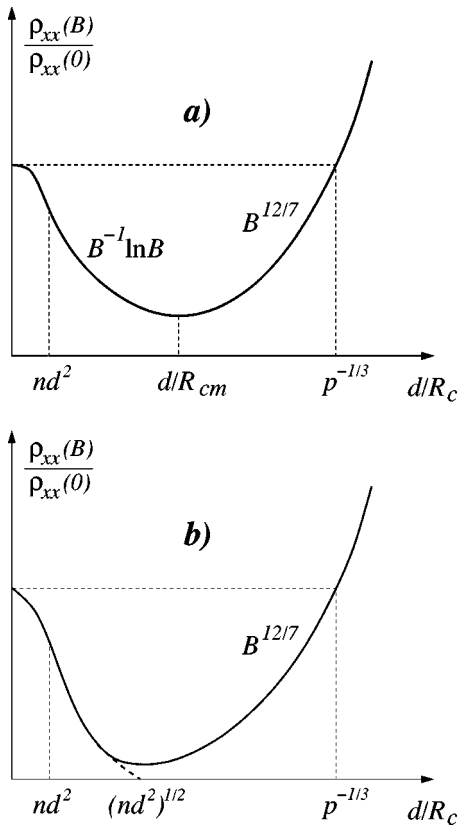

FIG. 5. Schematic behavior of $\rho_{xx}(B)$ as a function of d/R_c for intermediate magnetic fields at large p and $(d/l_L)^{1/3}\ll nd^2\ll p^{-1/3}$ for (a) $d/R_{cm}\ll(nd^2)^{1/2}$ and (b) $d/R_{cm}\gg(nd^2)^{1/2}$. The position of the minimum of $\rho_{xx}(B)$ in (a) is given by $d/R_{cm}\sim p^{-4/19}[nd^2\ln(1/nd^2p^{1/3})]^{7/19}$. Decreasing n leads to the nonmonotonic dependence of $\rho_{xx}(B)$ (cf. Fig. 3, where $n\to\infty$). The dashed line in (b) shows the behavior of $\rho_{xx}(B)$ given by Eq. (23).

implicitly assumed that there exists a range of B within which the percolative contribution is smaller than that given by Eq. (22). Indeed, since the percolative MR grows with increasing B (see Fig. 3), n should be small enough for the $B^{-1}\ln B$ falloff not to be masked by the percolation. Let us formulate the condition for the existence of the minimum in the dependence of $\rho_{xx}(B)$ for $p\gg1$. If one neglects (as everywhere in this section) the nonadiabatic decay of drift trajectories, the condition is $nd^2\ll p^{-1/3}$, as can be seen from Fig. 5(a). By matching Eqs. (22) and (15) we find that the minimum occurs at $R_c\sim R_{cm}$, where $d/R_{cm}\sim p^{-4/19}[nd^2\ln(1/nd^2p^{1/3})]^{7/19}$. We will show in Sec. III E, by taking the nonadiabatic decay into account, that the condition for the existence of the minimum actually reads $\max\{nd^2,(d/l_L)^{1/3}\}\ll p^{-1/3}$, which means that Fig. 5(a) correctly describes the MR if $(d/l_L)^{1/3}\ll nd^2$.

To conclude this section, note that the interval of validity of Eq. (22) shrinks to zero if $R_c/d\lesssim1$ and therefore the above considerations describe the behavior of the MR only for $nd^2\ll1$. According to Fig. 5, for large p the nonmonotonic behavior of $\rho_{xx}(B)$ develops for $nd^2\ll1$. In the case of small p the picture is similar but the parameter δ/a becomes relevant, which will be considered in Sec. IV.

D. Metal-insulator transition

As noted above, the validity of the derivation of Eq. (22) requires that $nR_c^2 \gg 1$. This condition appears already in the Lorentz model: if the opposite inequality is satisfied, the system without long-range inhomogeneities would be insulating ($\rho_{xx}=0$). In the presence of long-range disorder, the percolation mechanism of transport prevents ρ_{xx} from vanishing even at small nR_c^2. However, the parameter nR_c^2 determines the interval of B where the nontrivial mechanism of diffusion that leads to Eq. (22) is operative, namely $1 \ll nR_c^2 \ll R_c/d$. At $nR_c^2 \lesssim 1$, this mechanism is switched off in a manner inherent in a continuous phase transition by formation of disconnected clusters of trajectories, very much similar to the metal-insulator transition in the Lorentz model.[24,25] Hence the ''short scale'' (as opposed to the percolative) MR [Eq. (22)] behaves near the transition according to

$$\frac{\rho_{xx}(B)}{\rho_0} = (nd^2)^{1/2} \ln\frac{1}{nd^2} G\left(\frac{B_c - B}{B_c}\right), \tag{23}$$

where $G(x) \sim x^t$ vanishes as a power law at $x \to 0$ on the conducting side. The critical point $B=B_c$ corresponds to the critical concentration $n=n_c \sim R_c^{-1/2}$. This behavior of $\rho_{xx}(B)$ is shown in Fig. 5(b). Comparing Figs. 5(a) and 5(b), we see that the critical falloff (23) is not masked by the percolation provided $(nd^2)^{1/2} \ll d/R_{cm}$. If this condition is satisfied, the minimum in the dependence of $\rho_{xx}(B)$ occurs at $nR_c^2 \sim 1$.

We conjecture that the exponent t in the function $G(x)$ can be found by mapping the problem of percolation of skipping cyclotron orbits onto that of percolation of the electric current through an ensemble of conducting circles of radius R_c scattered randomly with the density n (note that two rosette orbits of radius $2R_c$ do not mix with each other if the distance between the centers of the rosettes exceeds $2R_c$). The latter problem belongs to the universality class of a two-dimensional percolation with a finite threshold, for which many critical exponents are known (see, e.g., Ref. 35; it is worth noting that the percolation of drift trajectories considered above does not belong to this class). In particular, the fraction of space occupied by the infinite cluster of connected circles vanishes near the threshold as $(n-n_c)^\beta$ with $\beta \simeq 0.14$, whereas the conductivity through the infinite cluster exhibits a power-law behavior with the critical exponent $t \sim 1.2$.

E. Nonadiabatic decay

In Sec. III C, we inferred the $B^{-1}\ln B$ falloff of $\rho_{xx}(B)$ [Eq. (22)] by assuming that the drift picture is applicable in the whole range $nR_c d \ll 1$. This is legitimate if $n\tilde{R}_c d \gg 1$, where $\tilde{R}_c$ is defined in Eq. (10). Otherwise the Drude value of $\rho_{xx}=\rho_0$ holds with increasing B up to the field where the adiabatic dynamics starts and there is an exponentially fast crossover between $\rho_{xx}=\rho_0$ and ρ_{xx} given by Eq. (22), which is governed by the nonadiabatic scattering.

Let D_{na} be the diffusion coefficient across drift trajectories due to their nonadiabatic mixing. Since the rate of nonadiabatic transitions depends exponentially on the parameter d/δ and is therefore locally a wildly fluctuating quantity, we should be more specific here: we define D_{na} through a typical time d^2/D_{na} that it takes to change two typical drift trajectories of size $\sim d$ separated by a distance $\sim d$ (for thus defined diffusion coefficient $\ln D_{na}$ scales as d/δ, see, e.g., Refs. 30 and 5). If $n\tilde{R}_c d \ll 1$, a particle which initially resides on a ring with no AD will reach a ring containing one in a time

$$\tau_{na} \sim (d^2/D_{na})/nR_c d. \tag{24}$$

Then there are two possibilities. If $\tilde{\tau}_S \ll d^2/D_{na}$ [with $\tilde{\tau}_S$ defined by Eq. (18)], the particle will hit this AD, so that collisions with different AD's will occur at a rate $\sim \tau_{na}^{-1}$, which yields a contribution to the macroscopic diffusion coefficient $D \sim R_c^2/\tau_{na} \sim D_0 D_{na} \tilde{\tau}_S/d^2$, i.e.,

$$D \sim D_0 \frac{D_{na} R_c}{v_F d a}. \tag{25}$$

Note that D in this regime is proportional to a product of two diffusion coefficients, D_0 and D_{na}. If, by contrast, $\tilde{\tau}_S \gg d^2/D_{na}$, the particle will miss this AD and will go on exploring phase space in a chaotic way, which gives $D=D_0$. Since d^2/D_{na} at $R_c \sim \tilde{R}_c$ is of the order of the cyclotron frequency v_F/R_c, the crossover between these two regimes takes place with increasing B when $R_c \ll \tilde{R}_c$, (logarithmically) deep in the drift regime. Hence, if $n\tilde{R}_c d \ll 1$, the nonadiabatic decay of drift trajectories stretches the region of a chaotic diffusion to the point at which $D_{na}\tilde{\tau}_S/d^2 \sim 1$, which occurs at d/R_c only logarithmically larger than $(d/l_L)^{1/3}$. At larger B, the resistivity starts to fall off sharply, according to Eq. (25), until $D_{na}\tilde{\tau}_S/d^2$ becomes of order $nR_c d \ln(1/nR_c d)$, where this exponential behavior crosses over into the power-law falloff described by Eq. (22). The characteristic features in the behavior of $\rho_{xx}(B)$ at $p \gg 1$ associated with the nonadiabatic decay of drift trajectories are illustrated in Fig. 6 for the range of B which corresponds to the falloff of $\rho_{xx}(B)$ in Figs. 5(a) and (b). At the point $d/R_c \sim (d/l_L)^{1/3}$ shown in Fig. 6, the adiabatic localization starts to develop.

Comparing Figs. 5(a), (b), and 6 one can formulate the condition for the existence of the dip in the dependence of the MR on B for $p \gg 1$. If $nd^2 \gg (d/l_L)^{1/3}$, the dip exists in the case of $nd^2 p^{1/3} \ll 1$, as in Figs. 5(a) and (b). If, by contrast, $nd^2 \ll (d/l_L)^{1/3}$, the nonmonotonic behavior in $\rho_{xx}(B)$ shows up for $dp/l_L \ll 1$. Figure 6 illustrates the behavior of $\rho_{xx}(B)$ in the case when the adiabaticity of motion in the long-range potential starts with increasing B well before the crossover to the percolative growth of $\rho_{xx}(B)$. This is the case at $(d/l_L)^{1/3} \ll \min\{d/R_{cm}, (nd^2)^{1/2}\}$. It is clear, however, that the above considerations of the nonadiabatic decay are equally valid for the case when the opposite inequality is satisfied. The only difference is that, if $(d/l_L)^{1/3} \gg \min\{d/R_{cm}, (nd^2)^{1/2}\}$, the exponential falloff of $\rho_{xx}(B)$ crosses over into the percolative growth directly, without passing through the intermediate $B^{-1}\ln B$ regime.

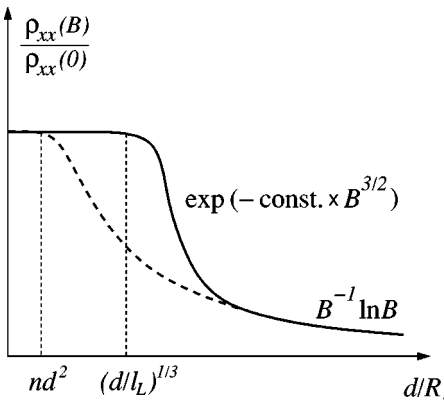

FIG. 6. Schematic representation of the behavior of $\rho_{xx}(B)$ at $nd^2 \ll (d/l_L)^{1/3} \ll p^{-1/3} \ll 1$ for moderately strong B which correspond to the falloff of $\rho_{xx}(B)$ in Figs. 5(a) and (b). The thick dashed line shows $\rho_{xx}(B)$ without taking the nonadiabatic decay of drift trajectories into account. Provided $nd^2 \ll (d/l_L)^{1/3}$, the nonadiabatic transitions stretch the range of B where $\rho_{xx}(B) \simeq \rho_0$. Beyond this range, $\rho_{xx}(B)$ falls off exponentially with increasing B until this falloff crosses over into the $B^{-1}\ln B$ behavior.

IV. STRONG MAGNETIC FIELD: RENORMALIZATION OF THE COLLISION TIME

Now let us turn to the extreme of strong B, where the parameter δ/a becomes relevant. As will be shown below, the effect of small δ/a is twofold. First, the time τ_S' between collisions with two different AD's for particles drifting along percolative trajectories (which is τ_S at large enough δ/a, how large—see below) gets longer. Second, a typical hopping length R_h across the drift trajectory due to the scattering on an AD (which is R_c at $\delta/a \gg 1$) gets smaller. Therefore before calculating the MR at small δ/a we have to consider how the elementary scattering acts are modified. Below, Sec. IV A deals with the scattering time τ_S', Secs. IV B and IV C with the hopping length R_h. Section IV D studies the MR for small δ/a.

A. Effective scattering time

Let us start by considering the case $\delta/a \ll 1$. To find τ_S', notice that at $\delta/a \ll 1$ the length of the drift trajectory between collisions $L_S \sim v_d \tau_S'$ cannot depend on a, i.e., only the concentration n matters. In the simplest case $R_c \ll d$, the length L_S clearly obeys the equation

$$nL_S R_c \sim 1, \tag{26}$$

which is rewritten as

$$\tau_S' \sim \tau_S a/\delta. \tag{27}$$

At $R_c \gg d$, however, there are different regimes for τ_S'. Namely, Eq. (27) is valid for τ_S' at $R_c \gg d$ only as long as $L_S \ll d$, i.e., when the drift trajectory between two collisions can be approximated as a straight line. If $L_S \gg d$, which is the case at $nR_c d \ll 1$, the trajectory exhibits fractal dimensionality on the scale of L_S. Specifically, the length of the percolating trajectory L_S and the distance ξ_S from the starting point are related to each other by $\xi_S \sim d(L_S/d)^{4/7}$ [see Eqs. (7) and (8)], i.e.,

$$\xi_S \sim d(v_d \tau_S'/d)^{4/7}. \tag{28}$$

It follows that the cyclotron orbit passes many times through the same spatial regions, which increases the time τ_S'. Let first $L_S \gg d$ but $\xi_S \ll R_c$ [i.e., $d \ll L_S \ll d(R_c/d)^{7/4}$]. In this regime, ξ_S [in contrast to L_S in Eq. (26)] is of order $(nR_c)^{-1}$:

$$n\xi_S R_c \sim 1, \tag{29}$$

which gives

$$\tau_S' \sim \tau_S \frac{a}{\delta} \frac{1}{(nR_c d)^{3/4}}. \tag{30}$$

Now let $\xi_S \gg R_c$. To find τ_S' in this limit, one should solve the following auxiliary problem. Collect all closed equipotential contours of size of order $\xi_S \gg d$ within the area $\xi_S \times \xi_S$. They form a ''bundle'' of width

$$w_S \sim d(d/v_d \tau_S')^{3/7} \sim d(d/\xi_S)^{3/4}. \tag{31}$$

The characteristic area covered by this bundle is $S(w_S) \sim L_S w_S \ll \xi_S^2$. Now enlarge the area by adding all points that are within a distance $\Delta \gtrsim w_S$ of the initial bundle. Doing so we get a new bundle that occupies an area $S(\Delta)$. The question is what is $S(\Delta)$ at $\Delta \sim R_c$ for $\xi_S \gg R_c \gg d$. Clearly, $S(\Delta) \sim L_S \Delta$ as long as $\Delta \lesssim d$. However, at $\Delta \gg d$, the area should exhibit a scaling behavior $S(\Delta) \sim L_S d(\Delta/d)^x$ with a nontrivial exponent x. To find x, notice that at $\Delta \sim \xi_S$ we should have $S(\xi_S) \sim \xi_S^2$. Using the equation $L_S \sim d(\xi_S/d)^{7/4}$ we thus get $x = 1/4$. It follows that the area $S(R_c)$ scales at $R_c \gg d$ as $L_S d(R_c/d)^{1/4}$ [which can be represented as $\xi_S^2 (R_c/\xi_S)^{1/4}$ to see that most of space within the area $\xi_S \times \xi_S$ is left empty]. Since $\delta \ll a$, it is clear that if there is an AD in this area, it will be inevitably hit by the cyclotron orbit. Therefore the length L_S obeys the equation

$$nS(R_c) \sim 1, \tag{32}$$

which yields $L_S \sim (nR_c)^{-1}(R_c/d)^{3/4}$ and

$$\tau_S' \sim \tau_S \frac{a}{\delta} \left(\frac{R_c}{d}\right)^{3/4}. \tag{33}$$

We see that Eqs. (30) and (33) match each other at $R_c \sim n^{-1/2} \gg d$. On the other hand, Eqs. (27) and (33) match at $R_c \sim d$.

The above derivation of τ_S' at $\delta/a \ll 1$ shows that the increase of the scattering time as compared to the ''Drude time'' τ_S is due to multiple passages of the cyclotron orbit through the area $a \times a$. Clearly, at $R_c/d \ll 1$ no renormalization of the scattering time occurs as long as $\delta/a \gg 1$. However, for $R_c/d \gg 1$ the scattering time is renormalized with increasing B already at some $\delta/a \gg 1$. Indeed, let $\delta/a \gg 1$ and consider the case $L_S \gg d$, $\xi_S \ll R_c$. The drifting cyclotron orbit experiences $L_S/\xi_S \gg 1$ returns to the area $d \times d$ and each time it probes the fraction $a/\delta \ll 1$ of space within this area.

One sees that if the product of the two factors $(L_S/\xi_S)\times(a/\delta)\gg 1$, then the collision time is much larger than the Drude time τ_S and obeys Eq. (29), which yields Eq. (30). Therefore it is only when $\delta/a\gg(nR_c d)^{-3/4}\gg 1$ that $\tau_S'=\tau_S$. Similarly, if $\xi_S\gg R_c$, Eq. (33) is valid for all $\delta/a\lesssim(R_c/d)^{3/4}$.

Inspection of Eqs. (27), (30), and (33) shows that the dependence of τ_S'/τ_S on B is parametrized by two parameters. In addition to p [Eq. (13)], it is convenient to introduce the parameter

$$\eta = n d^2 p, \tag{34}$$

which can be rewritten as $V_0 d/\epsilon_F a$, where V_0 is a characteristic amplitude of fluctuations of the long-range potential, ϵ_F the Fermi energy. The meaning of this parameter is that it describes the position of the crossover $\delta/a\sim 1$ in terms of the ratio d/R_c. Specifically, if $\eta\ll 1$, the crossover occurs at $d/R_c\sim\eta^{2/3}$, whereas if $\eta\gg 1$, at $d/R_c\sim\eta^{1/2}$. Note that the crossover point at $\eta\gg 1$ corresponds to $R_c\gg a$ [namely $R_c/a\sim(dl_L/a^2)^{1/4}$], however large η is. We thus have

$$\frac{\tau_S'}{\tau_S} = h\left(\frac{d}{R_c}, p, \eta\right). \tag{35}$$

By changing η with p held constant, we change the concentration n at a fixed mean free path l_S. In Sec. III B, we have already studied the limit $\eta\to\infty$: in that case the scattering time is not renormalized, so that $\tau_S'/\tau_S=1$ for all B independently of p. However, Eqs. (27), (30), and (33) tell us that at any finite η there exists a magnetic field above which τ_S'/τ_S starts to grow with increasing B. The function $h(x,p,\eta)$ which describes this growth reads

$$h(x,p,\eta) \sim \begin{cases} x^2\eta^{-1}, & x\gg\max\{\eta^{1/2},1\}; \\ x^{3/2}\eta^{-1}, & \eta^{2/3}\ll x\ll\min\{\eta p^{-1},1\}, \quad p^3\ll\eta\ll 1; \\ x^{9/4}p^{3/4}\eta^{-7/4}, & \max\{\eta p^{-1},\eta^{7/9}p^{-1/3}\}\ll x\ll\eta^{1/2}p^{-1/2}, \\ & \eta\ll\min\{p,p^{-3/5}\}; \\ x^{3/4}\eta^{-1}, & \max\{\eta^{4/3},\eta^{1/2}p^{-1/2}\}\ll x\ll 1, \\ & \eta\ll\min\{p,1\}. \end{cases} \tag{36}$$

The behavior of τ_S'/τ_S given by Eqs. (35) and (36) is illustrated in Fig. 7. One sees that in the limit of large B the collision time grows as B^2, whatever the parameters p and η. If $\eta\gg 1$, which corresponds to a sufficiently large concentration of AD's, this B^2 growth matches the Drude result directly [curves labeled by (i) in Figs. 7(a) and (b)]. In a more dilute array of AD's, there appear intermediate regimes, which proliferate as η is decreased [curves (ii)–(iv)]. Note that the smaller η for a given p, the sooner the renormalization of τ_S' starts with increasing B.

In Fig. 7(a), we marked the point $d/R_c\sim(d/l_L)^{1/3}$ which corresponds to the crossover between the diffusion and drift

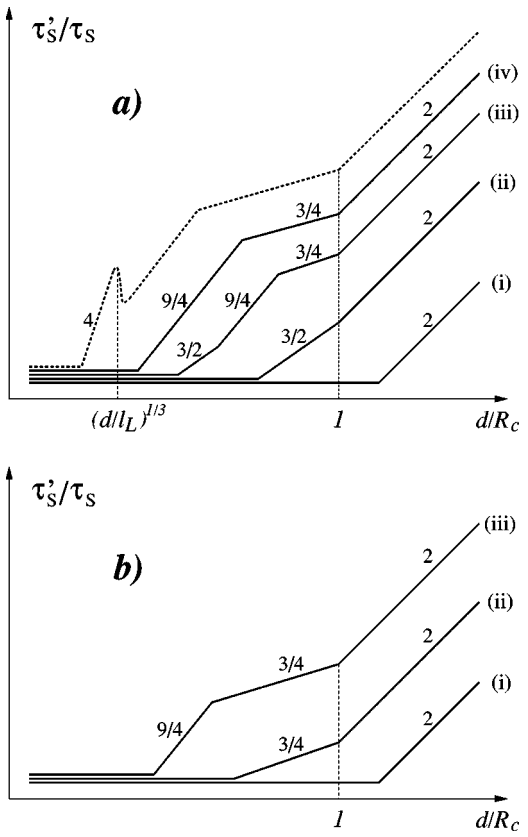

FIG. 7. Schematic behavior of τ_S'/τ_S as a function of d/R_c on a log-log scale for (a) $p\ll 1$ and (b) $p\gg 1$. The numbers denote the exponent of the power-law dependence of τ_S'/τ_S on B. Different curves in (a) illustrate how the dependence of τ_S'/τ_S on B for a fixed p is modified in different ranges of η: (i) $\eta\gg 1$; (ii) $p\ll\eta\ll 1$; (iii) $p^3\ll\eta\ll p$; (iv) $\eta\ll p^3$. Similarly in (b): (i) $\eta\gg 1$; (ii) $p^{-3/5}\ll\eta\ll 1$; (iii) $\eta\ll p^{-3/5}$. The dashed line in (a) shows the behavior of τ_S'/τ_S for η so small that the renormalization of τ_S'/τ_S starts with increasing B already in the diffusive regime (see the text).

regimes [smaller and larger d/R_c respectively, see Eq. (10)]. Equations (35) and (36) describe the drift regime. However, as illustrated in Fig. 7(a) by the uppermost (dashed) curve, if the concentration n is sufficiently low, the collision time is renormalized already in the diffusive regime. Indeed, for small n, τ_S'/τ_S calculated for drifting electrons will be large at the crossover point to the diffusive regime. A similar effect takes place for large p as well [not shown in Fig. 7(b)]. In the diffusive regime, τ_S'/τ_S is still given by Eq. (29), the only difference is that now in place of Eq. (28) one should take

$$\xi_S\sim\delta(v_F\tau_S'/R_c)^{1/2}, \tag{37}$$

which describes the diffusive motion of the cyclotron orbit. Substituting this expression for ξ_S in Eq. (29) yields

$$\tau_S'\sim\tau_S\frac{l_L}{l_S}\frac{1}{(nR_c^2)^2}, \tag{38}$$

i.e., the collision time starts to grow as B^4 before entering the drift regime, as shown in Fig. 7(a) by the dashed line. In the diffusive regime, $\rho_{xx}(B)$ is related to τ_S' by $\rho_{xx}(B)/\rho_0 \sim \tau_S/\tau_S'$, which gives

$$\frac{\rho_{xx}(B)}{\rho_0} \sim \frac{l_S}{l_L}(nR_c^2)^2. \tag{39}$$

As follows from Eq. (38), the crossover to the B^4 behavior with increasing B occurs at

$$d/R_c \sim (nd^2)^{1/2}(l_S/l_L)^{1/4}. \tag{40}$$

Comparing Eq. (40) with $(d/l_L)^{1/3}$ we conclude that the crossover to the drift regime takes place at larger B if $nd^2 \ll (d/l_L)^{2/3}(l_L/l_S)^{1/2}$. If, however, the concentration n is high enough, so that the opposite inequality is met, the region of validity of Eqs. (38) and (39) shrinks away and no renormalization of τ_S occurs in the diffusive regime.

Note a sharp change in the behavior of τ_S'/τ_S at the crossover between the drift and diffusion regimes [Fig. 7(a)]. The mismatch is due to the difference in the fractal dimensionality of extended trajectories in the two regimes: self-avoiding drift trajectories percolate in a superdiffusive way and therefore explore the area faster. The sharp crossover has the form of an exponential falloff of τ_S'/τ_S, governed by rapidly developing adiabaticity of electron motion. If one compares the times τ_S' obtained for the two (diffusion and drift) regimes close to the crossover point $d/R_c \sim (d/l_L)^{1/3}$, one can see that for small n, namely for $nd^2 \ll (d/l_L)^{5/7}(l_L/l_S)^{4/7}$, the ratio $\tau_S'/\tau_S \gg 1$ on both sides. The dashed line in Fig. 7(a) illustrates just this case. It is possible, however, that n falls into the intermediate range $(d/l_L)^{5/7}(l_L/l_S)^{4/7} \ll nd^2 \ll (d/l_L)^{2/3}(l_L/l_S)^{1/2}$, in which case τ_S' changes with increasing B in the following way: it first starts to grow in the diffusive regime, then, after the crossover into the drift regime, returns to the unrenormalized value τ_S, and only with further increasing B begins to grow again.

At this point it is worth emphasizing once more that, while in the diffusion regime all electrons behave in a similar way and τ_S' given by Eq. (38) is characteristic to all electrons, upon crossover into the drift regime the electrons find themselves divided into different groups, characterized by different collision times (the groups are mixed up only due to slow nonadiabatic dynamics). Specifically, τ_S' in Eq. (30) is the collision time for electrons that move along extended (percolative) drift trajectories. This time is renormalized even for $\delta \gg a$. On the other hand, electrons that upon crossover to the drift regime find themselves on typical drift trajectories of size $\sim d$ either do not collide with AD's at all, and for them the collision time is infinite (actually, provided they experience nonadiabatic transitions, the collision time is finite but exponentially large, as shown in Sec. III E), or are characterized by the unrenormalized collision time τ_S (at $\delta \gg a$), as explained in Sec. III C. Hence the renormalization of the collision time that we have analyzed in this section will affect the percolative contribution to the MR, which we will study in Sec. IV D. For $\delta \ll a$, the renormalization of τ_S will strongly affect also the short-scale dynamics of electrons residing on typical trajectories of size d, which will be considered in Sec. IV E.

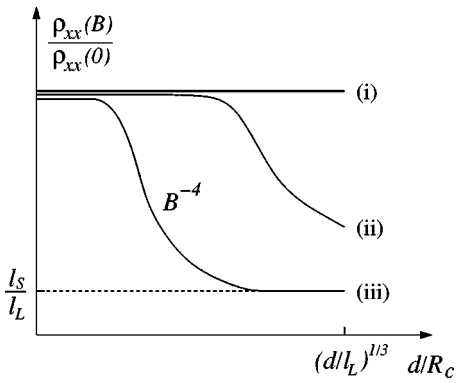

FIG. 8. Schematic behavior of $\rho_{xx}(B)$ as a function of d/R_c in the diffusive regime $d/R_c \ll (d/l_L)^{1/3}$. Different curves illustrate the dependence of $\rho_{xx}(B)$ on B in different ranges of n: (i) $nd^2 \gg (d/l_L)^{2/3}(l_L/l_S)^{1/2}$; (ii) $(d/l_L)^{2/3} \ll nd^2 \ll (d/l_L)^{2/3}(l_L/l_S)^{1/2}$; (iii) $nd^2 \ll (d/l_L)^{2/3}$.

Now let us return to the diffusive regime. Clearly, Eq. (38) is only valid as long as $v_F\tau_S' \ll l_L$, which is rewritten as $nR_c^2 \gg 1$. If the opposite limit, $nR_c^2 \ll 1$, is realized with increasing B still in the diffusive regime [which is the case for a very dilute array of AD's, namely for $nd^2 \ll (d/l_L)^{2/3}$], in this limit the scattering on AD's stops playing any role for diffusive electrons. The collision time is then given by l_L/v_F and

$$\rho_{xx}(B)/\rho_0 = l_S/l_L \tag{41}$$

does not depend on B, whereas τ_S'/τ_S keeps growing with increasing B. Yet, the scattering on AD's will become relevant again with further increasing B, once the system crosses over into the drift regime (where the scattering on AD's will prevent the adiabatic localization from completely suppressing the MR, as explained above). This behavior corresponds to the case when the crossover to the diffusive regime with decreasing B occurs not in the region of $B^{9/4}$ behavior, as shown in Fig. 7(a), but in the $B^{3/4}$ region. The overall behavior of the MR in the diffusive regime is illustrated in Fig. 8. We consider the effect of the renormalization of τ_S for diffusive electrons in detail elsewhere.[36]

As mentioned above, another effect of small δ/a is a renormalization of the hopping length for the diffusive dynamics across the drift trajectory due to the scattering on AD's, which we will consider in more detail below. Since both the effective scattering time and the hopping length are now modified, the shape of the MR is no longer parametrized by a single parameter. Specifically, we can replace f in Eq. (14) by a new function g which is given by

$$g(x,p) \sim \frac{\tau_S}{\tau_S'} f\left(x, p\frac{\tau_S'}{\tau_S}\right), \tag{42}$$

in the ''one-hop'' regime [cf. Eqs. (15) and (16)], while in the advection-diffusion regime [cf. Eq. (17)] we now have

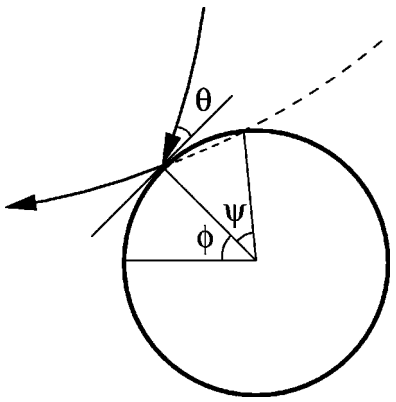

FIG. 9. Geometry of scattering of a skipping cyclotron orbit on an antidot: θ is the angle of incidence, ϕ the polar angle of the point at which the collision occurs, ψ the incremental increase of the angle ϕ between two consecutive collisions.

$$g(x,p)\sim\frac{\tau_S}{\tau_S'}\left(\frac{R_h}{R_c}\right)^{6/13}f\left(x,p\,\frac{\tau_S'}{\tau_S}\right). \tag{43}$$

A crossover between the two regimes occurs at $v_d\tau_S'\sim L(R_h)$, where $L(w)$ is defined in Eq. (7). The ratio τ_S'/τ_S is given by Eqs. (35) and (36). The ratio R_h/R_c will be calculated in Secs. IV B and IV C.

B. Skipping orbits

In Sec. IV A, we derived general expressions for the percolative MR for small δ/a in terms of τ_S' and R_h and calculated the effective scattering time τ_S'. Let us now evaluate R_h. The scattering problem for a cyclotron orbit that collides with a hard disc is nontrivial at $\delta/a\ll 1$. To begin with, notice that at $\delta/a\ll 1$ the drifting cyclotron orbit first hits the disc boundary at a small angle $\theta_1\ll 1$ (see Fig. 9). A simple geometric consideration yields a characteristic θ_1 for a particle incident on the disc with a drift-shift vector $\boldsymbol{\delta}$ (i.e., with a drift velocity $\boldsymbol{\delta}v_F/2\pi R_c$):

$$\theta_1\sim\left(-\frac{\boldsymbol{\delta}\cdot\mathbf{e}}{a}\right)^{1/2}\left(\frac{R_c+a}{R_c}\right)^{1/2}, \tag{44}$$

where **e** is the unit vector normal to the surface of the disc at the point of the collision. One sees that the angle of incidence vanishes when we let $\delta\to 0$, so that the skipping cyclotron orbit in effect starts to ''roll over'' the disc. Clearly, if it were not for the drift during the rollover, the collision angle θ would be conserved, being the same each time the particle returns to the disc after one cyclotron revolution. Therefore, although the drift is slow, in the sense that the typical hopping length for the guiding center after one collision $\sim R_c\theta\gg\delta$, it is because of the drift during the skipping process that the particle eventually breaks away from the AD. The length R_h is then understood as a shift of the guiding center at the point of the breakaway with respect to the equipotential contour along which it was drifting right before the first hit.

Since $\delta/a\ll 1$, we can treat the drift during the rollover perturbatively. The system of equations that describe the skipping in the absence of drift is given by

$$\phi_{n+1}=\phi_n+\psi(\theta_n); \tag{45}$$

$$\theta_{n+1}=\theta_n, \tag{46}$$

where ϕ_n is the polar angle (along the surface of the disc) defining the point of the nth collision, θ_n the collision angle, see Fig. 9. The function $\psi(\theta)$ obeys the equation $R_c\sin(\theta-\psi/2)=a\sin(\psi/2)$, which reduces to the linear relation

$$\psi(\theta)=\frac{2R_c}{R_c+a}\,\theta \tag{47}$$

in the limit of small θ. Equation (46) says θ is the integral of motion for the skipping process without drift. In the presence of drift, θ_n acquires an n-dependent correction $\Delta\theta_n=\theta_{n+1}-\theta_n$. To first order in δ the correction reads

$$\Delta\theta_n\simeq-\frac{R_c+a}{R_ca}\,\frac{\boldsymbol{\delta}_n\mathbf{e}(\phi_n)}{\theta_n}, \tag{48}$$

where $\boldsymbol{\delta}_n$ is the drift shift between the nth and $(n+1)$st collisions, $\mathbf{e}(\phi_n)$ the unit vector perpendicular to the surface of the disc at the point of the nth collision. Transforming to the continuous limit we get the differential equation

$$\frac{\partial\theta^2}{\partial\phi}=-\frac{2}{\psi(\theta)}\,\frac{R_c+a}{R_ca}\boldsymbol{\delta}(\phi)\mathbf{e}(\phi), \tag{49}$$

whose solution, after substituting $\psi(\theta)$ from Eq. (47), yields

$$\theta^3(\phi)=\theta^3(\phi_i)-\frac{3}{2a}\left(\frac{R_c+a}{R_c}\right)^2\int_{\phi_i}^{\phi}d\phi'\,\boldsymbol{\delta}(\phi')\mathbf{e}(\phi'). \tag{50}$$

The function $\boldsymbol{\delta}(\phi)$ in Eqs. (49) and (50) gives the drift shift for the cyclotron orbit whose guiding center is a distance R_c+a from the center of the disc in the direction specified by the angle ϕ. In fact, the integration in Eq. (50) runs along the guiding-center trajectory during the rollover, which is the contour $\rho=R_c+a$, where $\boldsymbol{\rho}$ is the radius vector counted from the center of the disc. Note that the integral term in Eq. (50) is bounded from above by $\sim\delta/a$ at $R_c\gg a$ and by $\delta a/R_c^2\sim a/(dl_L)^{1/2}$ otherwise. In both limits the maximum value of $\theta\ll 1$, which justifies the linearization (47) and our using of the term ''rollover.''

If we take ϕ_i in Eq. (50) equal to the polar angle at which the cyclotron orbit hits the disc for the first time, then $\theta(\phi_i)$ should be put to zero in the continuous approximation. With the same accuracy the angle ϕ_f at which the breakaway occurs satisfies the condition $\theta(\phi_f)=0$. According to Eq. (50), we can recast the latter condition as

$$\int_{\phi_i}^{\phi_f}d\phi\,\boldsymbol{\delta}(\phi)\mathbf{e}(\phi)=0. \tag{51}$$

This equation yields ϕ_f as a function of ϕ_i and, consequently, enables us to determine the shift R_h. Let us intro-

duce an effective random potential $V(\boldsymbol{\rho})$ as the average of the real potential over the cyclotron orbit with the guiding center at the point $\boldsymbol{\rho}$ [at $R_c \ll d$ the two potentials almost coincide, but at $R_c \gg d$ a typical amplitude of fluctuations of the effective potential $V(\boldsymbol{\rho})$ with the same correlation radius d is obviously $\sim (R_c/d)^{1/2}$ times smaller]. The drift occurs along equipotential lines of $V(\boldsymbol{\rho})$. Since the shift $\boldsymbol{\delta}(\boldsymbol{\rho}) \propto \nabla V(\boldsymbol{\rho}) \times \mathbf{e}_z$, where $\mathbf{e}_z$ is the unit vector along the magnetic field, Eq. (51) is rewritten as

$$\int_{\phi_i}^{\phi_f} d\phi (\nabla V \times \mathbf{e}_z) \cdot \mathbf{e}(\phi) = 0, \tag{52}$$

which, for the integration along the arc $\rho = R_c + a$, finally gives

$$V(\rho, \phi_f) - V(\rho, \phi_i) = 0. \tag{53}$$

We thus see that in the limit of small δ/a the cyclotron orbit, having skipped along the surface of the hard disc, breaks away on the equipotential contour with the same V as it had before hitting the disc, i.e.,

$$R_h = 0 \tag{54}$$

in the continuous approximation. Note that for the drift in a homogeneous electric field, when $\boldsymbol{\delta}(\boldsymbol{\rho}) = \text{const}$, this result follows straightforwardly from symmetry of the scattering problem. What Eq. (53) tells us is that, remarkably, R_h vanishes in the case of varying $V(\boldsymbol{\rho})$ as well.

Let us compare the above picture with a familiar example of adiabaticity of scattering on a smooth inhomogeneity $V(\boldsymbol{\rho})$: in that case, the vanishing of R_h simply means that the guiding center drifts along a locally perturbed equipotential line of $V(\boldsymbol{\rho})$. Naively, one might think that a collision with the disc destroys the adiabaticity since the impenetrable hard disc makes a part of the equipotential line of $V(\boldsymbol{\rho})$ inaccessible. However, as follows from Eq. (53), the skipping of the cyclotron orbit around the disc goes on adiabatically, provided δ/a is infinitesimally small, and the result $R_h = 0$ still holds.

C. Nonadiabatic skipping

The zero result for R_h was obtained in Sec. IV B by treating the drift during the rollover perturbatively, to first order in δ/a, and by taking the continuous limit. To find R_h, we should now relax this approximation. Before doing so, it is worthwhile to recall how R_h behaves for scattering on a smooth inhomogeneity. In that problem, it is known that taking higher gradient terms into account does not lead to a finite R_h and, in fact, the problem of finding R_h does not allow for any perturbative solution that could be expanded in powers of the parameter $\delta/d \ll 1$, where d is a characteristic size of the inhomogeneity. Specifically, for a smooth inhomogeneity, R_h is exponentially small at $\delta/d \ll 1$ (see, e.g., Ref. 34 for a solution of the scattering problem and references therein). As we have shown above, the case of a hard disc placed in a smoothly varying environment is similar in that the scattering is also almost adiabatic at $\delta/a \ll 1$. A question then arises if the nonadiabatic scattering that leads to a finite R_h is also exponentially suppressed. The answer is no, since there is an important difference between the two cases. Namely, the approximation within which the skipping of the cyclotron orbit can be considered as a continuous adiabatic process [Eq. (49)] fails completely near the points $\phi = \phi_i$ and $\phi = \phi_f$. Indeed, near these points dynamics of the collision angle $\theta(\phi)$ is nonadiabatic since θ is close to zero, so that $\Delta\theta_n$ is of order θ_n itself and the expansion (48) is not valid any more. A finite shift R_h is therefore due to the discreteness and incommensurability of the skipping along the sharp boundary of the hard disc. It is given by the elementary (associated with a single collision) hopping length of the guiding center near $\phi = \phi_{i,f}$, which is $R_{h1} \sim (R_c + a)\psi(\theta_1)$. Substituting θ_1 from Eq. (44) we finally get for a characteristic amplitude of the shift

$$R_{h1} \sim R_c \left(\frac{\delta}{a} \frac{R_c + a}{R_c} \right)^{1/2}. \tag{55}$$

We see that, in contrast to the case of a smooth inhomogeneity, R_{h1} scales as a power of δ, namely $R_{h1} \propto \delta^{1/2}$. Note also that the characteristic scale d, on which the smooth $V(\boldsymbol{\rho})$ changes, appears in Eq. (55) only through the drift shift δ.

Equation (55) describes a single scattering in which the particle breaks away from the disc along an equipotential with V almost equal to that of the equipotential along which it is incident on the disc. Using Eq. (55), dynamics of skipping orbits in the limit $R_c \ll d$ can be understood quite straightforwardly. Since in this limit the drift is almost homogeneous in the course of skipping, for a given V there is typically only one equipotential line that crosses the guiding-center trajectory during the rollover. Accordingly, if it were not for the small shift (55), the particle would simply continue to drift after the rollover along the same equipotential line. The picture becomes far more complicated at large $R_c \gg d$ since in that case there are many equipotential lines with the same V that intersect the guiding-center trajectory corresponding to the rollover.

Let $R_c \gg d$. In this limit, one should distinguish two regimes according to whether the typical hopping length after one collision $R_{h1} \sim R_c(\delta/a)^{1/2}$ [Eq. (55)] is larger or smaller than d. Consider first the case $R_{h1} \ll d$, i.e., let $d \ll R_c \ll d(a/\delta)^{1/2}$. The characteristic number of equipotential lines with the same V that cross the circle of radius $\rho = R_c + a$ around the disc (which is the guiding center trajectory in the course of skipping) is of order $R_c/d \gg 1$. Clearly, the direction of drift (to or away from the surface of the disc) alternates during the skipping. It follows that the particle which started skipping will break away along the equipotential line that is the first to cross the guiding-center trajectory corresponding to the skipping. Yet, since the equipotential lines are closed loops (typically of size d), the particle will come full circle and return to the disc (see Fig. 10). Then the process will repeat itself with other equipotential lines along the surface of the disc. We have assumed, however, that the particle is incident on the disc along a percolating extended trajectory. Therefore the multiple returns will stop when the particle picks up this trajectory.

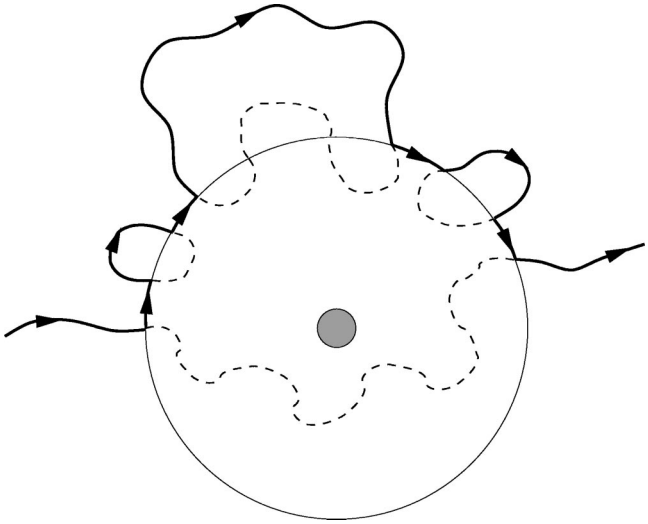

FIG. 10. Schematic picture of scattering of a cyclotron orbit on an antidot at $\delta \ll a$, $R_c \gg d$ and $R_{h\Sigma} \ll w_S$. The thick solid line with arrows is the guiding-center trajectory. The dashed lines are equipotential contours which cannot be accessed by the guiding center. The small shaded circle in the center of the figure shows the antidot. The thin circle of radius $R_c + a$ around it is the boundary of the area impenetrable for the guiding center. The parts of the guiding-center trajectory that coincide with this boundary correspond to skipping of the cyclotron orbit, which alternate with parts corresponding to drift. The drift occurs between each breakaway from the antidot and consecutive return to it.

Let us evaluate the total shift $R_{h\Sigma}$ with which the particle will finally break away. Elementary shifts for the repeating collisions are uncorrelated with each other, so that

$$R_{h\Sigma}^2 \sim R_{h1}^2 R_c \left[\int_d^{R_c} d\Lambda \, \Lambda \, W(\Lambda) \right]^{-1}, \tag{56}$$

where $W(\Lambda)$ is the probability density for the drift trajectory that broke away from the disc to hit it again, i.e., to cross the arc $\rho = R_c + a$, for the first time after the breakaway at a distance Λ from the starting point. It is instructive to map the problem of finding $W(\Lambda)$ onto a more conventional one by noting that the power-law scaling of $W(\Lambda)$ describes how a deposition rate for particles emitted by a point source and moving in two dimensions in the presence of an absorbing line falls off with increasing distance Λ along this line. If the particles would experience an uncorrelated diffusion with the elementary step $\sim d$, then it is straightforward to see, by solving the diffusion equation with the absorbing boundary, that $W(\Lambda) \sim d/\Lambda^2$. In fact, one can show, by introducing a scale-dependent diffusion coefficient which describes the drift, that this result holds for the drifting particles as well, i.e., $W(\Lambda)$ and $P(\xi)$ [Eq. (19)] have the same scaling behavior. Hence the integral in Eq. (56) logarithmically diverges and the typical number of collisions before the final breakaway is $R_c/d \ln(R_c/d)$. It follows that

$$R_{h\Sigma} \sim R_c \left[\frac{\delta}{a} \frac{R_c}{d \ln(R_c/d)} \right]^{1/2}. \tag{57}$$

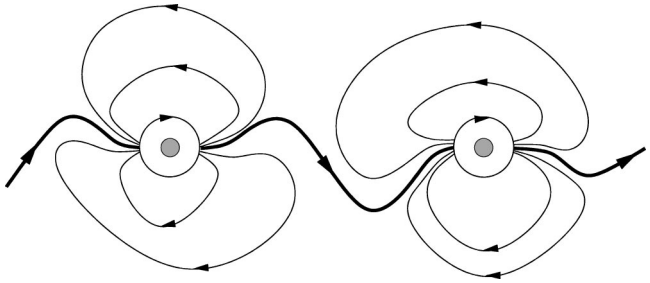

FIG. 11. Schematic picture of scattering of a cyclotron orbit on antidots at $\delta \ll a$, $R_c \ll d$ and $R_{h1} \gg w_S$. The line with arrows shows the guiding-center trajectory. The thicker line is the trajectory that takes the particle from one antidot to another (two of which are shown by shaded circles). Until the guiding center picks up this trajectory the particle is stuck to an antidot and keeps colliding with it, by making long drift excursions between the collisions. For $R_c \gg d$, the scattering process can be visualized as a ''combination'' of Figs. 10 and 11.

Clearly, the necessary condition for the above derivation of $R_{h\Sigma}$ to be valid is $R_{h\Sigma} \ll d \ll R_c$, which means $d \ll R_c \ll d(a/\delta)^{1/3} \ln^{1/3}(a/\delta)$. It is worthwhile to mention that if $R_c \ll d(a/\delta)^{1/3}$ the characteristic hopping length for the skipping cyclotron orbit $R_c \psi_{max} \ll d$. Here $\psi_{max} \sim (\delta/a)^{1/3}$ is the maximum scattering angle for a single-run skipping at $R_c \gg a$ [see Eqs. (47) and (50)].

Now let R_{h1} be still smaller than d but let $R_{h\Sigma} \gg d$, i.e., consider the interval $d(a/\delta)^{1/3} \ln^{1/3}(a/\delta) \ll R_c \ll d(a/\delta)^{1/2}$. An essential difference appears in this regime: the shift accumulated through multiple breakaways and returns exceeds d before the rollover is finished. At this point it is worth recalling that the elementary shifts for each breakaway are accompanied by changes of V corresponding to drift trajectories. Accordingly, when the accumulated shift gets larger than d, the initial and current values of V become uncorrelated with each other. It is evident that we should treat this case separately, since now one cannot identify $R_{h\Sigma}$ given by Eq. (57) with a shift with which the particle has finally broken away never to return. This conclusion becomes even clearer when not only $R_{h\Sigma}$ but also R_{h1} [Eq. (55)] is larger than d, i.e., when $R_c \gg d(a/\delta)^{1/2}$. In the latter case, the memory about the initial value of V is lost already after one collision.

The picture emerging in the limit $R_{h\Sigma} \gg d$ signals that one should also fine tune the derivation of Eqs. (55) and (57). Namely, these equations should be supplemented with the condition under which the problem of finding R_h can in fact be formulated as the scattering problem for a *single* disc. Indeed, for a single disc, one actually cannot specify with which accuracy the particle should hit the vicinity of the percolating trajectory so as to be able to break away from the disc. To answer this question, we need to consider a scattering problem for *two* discs. Specifically, consider two discs separated by a typical distance $L_S \sim v_d \tau_S'$ measured along the percolating trajectory (Fig. 11). The two discs are connected by a bundle of drift trajectories of width w_S [Eq. (31)]. One sees that the particle will break away from one disc and get through to the other after a single rollover only if

$\max\{R_{h1},R_{h\Sigma}\}$ is within this width. If this condition is not satisfied, the cyclotron orbit will keep going around the disc until it happens that its guiding center hits the strip of width w_S at the same time when θ vanishes. It follows that at $R_c \ll d$ the shift is given by Eq. (55) only if $R_{h1} \ll w_S$. If, however, $R_{h1} \gg w_S$, it takes typically $N_r \sim R_{h1}/w_S$ revolutions around the disc before the particle breaks away and

$$R_h \sim w_S \tag{58}$$

in this limit. Similarly, at $R_c \gg d$ the shift R_h is given by Eq. (57) only if $R_{h\Sigma} \ll w_S$; otherwise, $R_h \sim w_S$ (the picture can be visualized as a ''combination'' of Figs. 10,11). For $R_c \gg d$, the number of revolutions around the disc N_r, necessary for the simultaneous tuning of V and θ corresponding to the breakaway, is different in three different regimes. Namely, $N_r \sim R_{h\Sigma}/w_S$ for $w_S \ll R_{h\Sigma} \ll d$, independently of the ratio R_{h1}/w_S. With increasing $R_{h\Sigma}$, if $R_{h\Sigma} \gg d$, we have $N_r \sim d/w_S$ as long as $R_{h1} \ll d$, and $N_r \sim R_{h1}/w_S$ otherwise. In particular, one sees that if $R_{h\Sigma} \gg d$, it always takes many revolutions before the breakaway occurs and the shift R_h is always determined by w_S.

D. Percolation in a dilute antidot array

In Sec. IV C, we discussed scattering of a drifting cyclotron orbit on a single AD at $\delta/a \ll 1$. Consider now the MR at $\delta/a \ll 1$. Let us start with the limit of a small concentration of AD's $n \to 0$. As outlined in Sec. II B, in the absence of AD's the conductivity at large B is only due to the exponentially weak nonadiabatic scattering on long-range disorder. Let us neglect this additional contribution to $\rho_{xx}(B)$ and calculate the contribution that is due to the scattering on very rare hard discs. We thus seek a term in $\rho_{xx}(B)$ which is proportional to a power of n at small n. Let $R_c \ll d$. Since at $n \to 0$ the bundle of drift trajectories that connect two discs becomes infinitesimally narrow [$w_S \propto n^{3/7}$ at $n \to 0$ according to Eqs. (27) and (31)], the particle sticks to a disc for a long time τ_{st} until it picks up a trajectory that is extended enough to take it to another disc. The number of the unsuccessful attempts to break away from the disc is given by $N_r \sim R_{h1}/w_S \gg 1$. To evaluate τ_{st}, notice that the sticking time is determined by a slow drift along the closed loops that repeatedly return the particle back to the disc, not by the fast skipping in between. However, most of the attempts end up in quick returns to the vicinity of the point of the first collision and so give only a small contribution to τ_{st}. We estimate τ_{st} as

$$\tau_{st} \sim \int_{w_S}^{R_{h1}} \frac{dw}{w_S} \frac{L(w)}{v_d}, \tag{59}$$

where $L(w)$ is given by Eq. (7). The integral is determined by $w \sim w_S$, which yields $\tau_{st} \sim \tau_S'$. We thus see that the effective scattering time between collisions with different discs is given by the drift time between the discs. Accordingly, the total distance passed by the particle in the multiple rollovers is typically of order L_S. In fact, this conclusion holds for the case $R_c \gg d$ as well. The only difference is that at large R_c the particle experiences multiple breakaways and returns on the scale of a single rollover. However, τ_{st} does not renormalize the characteristic time between collisions with different discs, which is given by τ_S', similarly to the case $R_c \ll d$.

We are now in a position to calculate the AD-induced contribution to the MR in the limit of small n. According to the picture above, the scattering on a given AD is over when the particle hits another AD separated by a distance $\xi_S \sim d(v_d \tau_S'/d)^{4/7}$, and the characteristic time between two scatterings is τ_S'. As long as we neglect the nonadiabatic corrections to the drift in the long-range potential, there is a clear separation between localized and extended drift trajectories. Only a small fraction of trajectories get delocalized by means of collisions with AD's, namely $\sim w_S L_S/\xi_S^2 \ll 1$. The diffusion coefficient of particles residing on these trajectories is $\sim v_d \xi_S^2/L_S$. We thus see that the macroscopic diffusion coefficient is given by Eq. (9) with a rescaled scattering time $\tau_S \to \tau_S'$, which yields the MR obeying Eq. (42).

It is worth noting that the dynamics of particles is essentially different at $n \to \infty$ (Sec. III B) and $n \to 0$, despite being described by similar equations. In the former case, there is a strong exchange, caused by collisions with AD's and governed by a detailed balance of scattering processes, between the stream of fast particles which follow the links of the percolation network and the reservoir of ''quasilocalized'' particles which stick for a long time to within the critical cells of the network. By contrast, at $n \to 0$ there is no such exchange and the drift trajectories within the cells of the percolation network are strictly localized. However, in both cases the MR is determined by the fast particles moving along the links of the percolation network, which is why it does not matter if the particles moving inside the critical cells are localized or not. Put another way, although the total number of delocalized particles decreases at $n \to 0$, this effect is compensated by more frequent crossings, due to collisions with AD's, of the percolative drift trajectory by particles that remain delocalized.

Substituting Eqs. (27) and (33) into Eq. (42) we get

$$\frac{\rho_{xx}(B)}{\rho_0} \sim p^{4/7} \eta^{3/7} \left(\frac{d}{R_c}\right)^{39/28} \tag{60}$$

for $R_c \gg d$ and

$$\frac{\rho_{xx}(B)}{\rho_0} \sim p^{4/7} \eta^{3/7} \left(\frac{d}{R_c}\right)^{4/7} \tag{61}$$

in the opposite limit. According to Eqs. (60) and (61), $\rho_{xx} \propto n^{3/7}$ at $n \to 0$.

One sees from Eq. (61) that ρ_{xx} taken in the limit $n \to 0$ behaves at large B as $B^{4/7}$. As compared to Eq. (17), which describes the asymptotic behavior in the hydrodynamic regime $n \to \infty$ and gives $\rho_{xx} \propto B^{10/13}$, the divergence of ρ_{xx} with increasing B is weakened, but is still present. However, neither of the two limiting cases (17) and (61) describes the asymptotics of the MR for $B \to \infty$ at a given finite n, which we discuss below.

Let us turn to the percolative MR in a denser array of AD's. Increasing n yields wider links of the percolation net-

work, so that eventually w_S becomes larger than the elementary shift $\max\{R_{h1},R_{h\Sigma}\}$ (Sec. IV C). This transport regime is described by the advection-diffusion Eq. (17) modified according to Eq. (43). Using Eqs. (55) and (57) for R_{h1} and $R_{h\Sigma}$, and Eqs. (27) and (33) for τ_S' in Eq. (43) gives

$$\frac{\rho_{xx}(B)}{\rho_0}\sim p^{10/13}\eta^{6/13}\left(\frac{d}{R_c}\right)^{1/52}\ln^{-3/13}\left(\frac{R_c}{d}\right) \tag{62}$$

for $R_c\gg d$ and

$$\frac{\rho_{xx}(B)}{\rho_0}\sim p^{10/13}\eta^{6/13}\left(\frac{R_c}{d}\right)^{2/13}\left(\frac{R_c+a}{R_c}\right)^{3/13} \tag{63}$$

for $R_c\ll d$.

The condition at which the ''one-hop'' percolation [Eqs. (60) and (61)] crosses over with increasing B into the advection-diffusion regime [Eqs. (62) and (63)] is given by somewhat cumbersome formulas: the crossover occurs at $d/R_c\sim(p^6\eta)^{3/125}\ln^{-21/125}(p^6\eta)$ for $p^6\eta\ll 1$, at $d/R_c\sim(p^6\eta)^{1/22}$ for $1\ll(p^6\eta)^{1/22}\ll d/a$, and at $d/R_c\sim(p^6\eta)^{1/15}(a/d)^{7/15}$ for $(p^6\eta)^{1/22}\gg d/a$.

Equation (63) tells us that the asymptotics of the MR at $B\to\infty$ is $\rho_{xx}\propto B^{1/13}$, i.e., the MR diverges as a power law in the limit of large B. However, this divergence is so weak that from a practical point of view it is indistinguishable from a saturation of $\rho_{xx}(B)$. Nonetheless, it is a remarkable fact that in the extreme $B\to\infty$ the MR in the presence of both AD's and a long-range potential does not go to zero, in contrast to Eqs. (1) and (4), which predict vanishing of ρ_{xx} when only one type of disorder is present.

E. Rosette orbits in the presence of weak drift

In Sec. IV D, we considered the percolative contribution to the MR at small δ/a. Now we proceed to the ''short-scale'' contribution associated with rosette states (Secs. II A and III C). Let us analyze how the Lorentz gas behavior is restored with decreasing strength of the smooth disorder. Since we deal with the case $a/d\ll 1$, the Lorentz model limit is achieved for a very weak long-range potential, such that at $R_c/l_S\sim 1$, when the falloff (1) starts, the scattering on the long-range potential is already strongly adiabatic. The condition of adiabaticity at $R_c/l_S\sim 1$ and $l_S/d\gg 1$ translates into $l_L/d\gg(l_S/d)^3$. As we will see below, the condition of the Lorentz gas falloff $\rho_x(B)\propto B^{-1}$ not being dominated by the contribution of ''hopping rings'' (Sec. III C) is much stronger, namely

$$l_L/d\gg(l_S/d)^3(d/a)^4. \tag{64}$$

The solution of the scattering problem for a single disc in Sec. IV B shows that at $\delta/a\ll 1$ there is a well-defined separatrix $\theta_{max}\ll 1$ for the angle of incidence θ in the phase space (θ,ϕ), which divides skipping cyclotron orbits into two groups, delocalized and localized. Namely, trajectories that will finally break away from the disc belong to the part of the phase space with $\theta<\theta_{max}$, whereas the region $\theta>\theta_{max}$ is filled with those that will never escape. In other words, almost the whole phase space is filled with bound states. According to Eq. (50), the critical angle

$$\theta_{max}\sim(\delta/a)^{1/3}[(R_c+a)/R_c]^{2/3}. \tag{65}$$

Indeed, a drifting cyclotron orbit that is incident on the disc both hits it for the first time and finally breaks away at $\theta\lesssim\theta_1$ [Eq. (44)], while reaching a maximum θ, which depends on the incident parameter but does not exceed θ_{max} given by Eq. (65), during a rollover in between.

Let us show that a particle which starts with some $\theta>\theta_{max}$ will not be able to break away. What is important to us is that in order to break away the particle has to decrease θ down to $\theta\sim\theta_1$. Suppose this might happen and the particle has escaped. Then we could consider a complementary scattering problem by reversing time and sending the particle that has broken away back to the disc. However, we know from Sec. IV B that for this scattering problem θ will never exceed θ_{max}. Hence we come to a contradiction which shows that the initial assumption about the possibility of a breakaway cannot be realized. We thus see that trajectories that started to skip along the disc with $\theta>\theta_{max}$ can never cross the boundary $\theta=\theta_{max}$ and so will remain bound to the disc. The fact that there exist bound states for magnetized electrons interacting with a single hard disc in the case of a homogeneous in-plane electric field was observed in the numerical simulation.[37]

The existence of the separatrix θ_{max} means that the contribution to $\rho_{xx}(B)$ of rosette states with $\theta>\theta_{max}$ is given by

$$\rho_{xx}(B)/\rho_0\sim R_c/l_S \tag{66}$$

for all $\delta/a\ll 1$ [cf. Eq. (1)].

Let us now compare two terms in $\rho_{xx}(B)$ that are associated with the short-scale diffusion at finite δ/a. One, described by Eq. (22), is due to the hopping of ''rings'' introduced in Sec. III C. The other, given by Eq. (66), is due to the hopping of rosette states. Note a similarity between the two mechanisms of transport: in both cases a particle interacts with a disc many times before changing to another disc. The comparison shows that the concentration of particles participating in the hopping-ring transport is much larger than that of rosette states. It is clear, however, that if we send $\delta\to 0$, the hopping rings should not contribute to $\rho_{xx}(B)$, which will be given by Eq. (1). It follows that there should exist yet another, intermediate regime of hopping, associated with the evolution of the hopping-ring transport with decreasing δ/a. To describe the latter, notice first of all that Eq. (22) stops to be valid already at some $\delta/a\gg 1$. Indeed, the logarithmic factor in Eq. (22) is associated with the drift along closed loops of size $\xi\lesssim(nR_c)^{-1}$. Therefore the derivation of Eq. (22) in fact implies that the time it takes to come full circle along the longest loop of size $\xi\sim(nR_c)^{-1}$ is smaller than $\tilde{\tau}_S(\xi)$ [Eq. (21)] for this ξ, which yields the condition $\delta/a\gtrsim(nR_cd)^{-3/4}\gg 1$. Note that this is the same condition at which the effective scattering time for $d\ll\xi_S\ll R_c$ in Sec. IV A is not renormalized by the parameter δ/a and is given by τ_S [cf. Eq. (30)]. At smaller δ/a, in the

interval $1 \ll \delta/a \ll (nR_c d)^{-3/4}$, only ξ in the range $1 \lesssim \xi/d \lesssim (\delta/a)^{4/3}$ contribute to ρ_{xx}, which gives

$$\rho_{xx}(B)/\rho_0 \sim nR_c d \ln(\delta/a). \tag{67}$$

This equation is valid with decreasing δ/a down to $\delta/a \sim 1$. At still smaller δ/a, the particle is scattered out by the same AD after passing a distance of order d. Accordingly, the characteristic time between changes of AD's in this regime increases due to the slowing down of the drift as $\tau_S a/\delta$. It follows that for $\delta/a \ll 1$,

$$\rho_{xx}(B)/\rho_0 \sim nR_c d\ \delta/a. \tag{68}$$

Equations (68) and (66) match each other at $\delta \sim a^2/d$ and we conclude that the regimes (67) and (68), intermediate between those described by Eqs. (22) and (66), occur in the interval $a/d \ll \delta/a \ll (nR_c d)^{-3/4}$. By requiring that δ at $R_c/l_S \sim 1$ is much smaller than a^2/d we arrive at the condition (64). The overall behavior of $\rho_{xx}(B)$ for the case of very weak long-range disorder is obtained by adding the short-scale contribution, described by Eqs. (22) and (66)–(68), and the percolative contribution analyzed in Sec. IV D. This leads to nonmonotonic behavior of the MR, such that $\rho_{xx}(B)$ first falls off with increasing B and then crosses over into the percolative growth.

V. NUMERICAL SIMULATION

We have solved numerically the classical equation of motion for a charged particle in a random array of hard discs in the presence of smooth disorder. In the numerical simulation, the latter is characterized by the correlator

$$\langle V(\mathbf{r})V(0)\rangle \propto \frac{1}{[1+(r/d)^2]^{3/2}} \tag{69}$$

with the ratio $d/a \simeq 21.5$. The concentration n of the isolated scatterers has been chosen such that they make an important contribution to the resistance at zero magnetic field. Specifically, $\pi n d^2 \simeq 6.2$ and $l/l_S \simeq 0.58$, where l is the total mean free path and $l_S = 3/8na$.

In Fig. 12 we present the MR data for our model system. Since the characteristic values of the magnetic field (given in the figure caption in terms of the parameter d/R_c) are rather close to each other, it has not been possible to unambiguously separate different regimes. Yet, the nonmonotonic behavior of $\rho_{xx}(B)$, predicted by the theoretical analysis, is clearly seen. Note that the size of the error bars at $d/R_c \gtrsim 5$ denotes only the statistical uncertainty. In addition to the latter, there is a systematic uncertainty originating from a very slow guiding-center motion in the large-B limit, which makes it difficult to observe the true diffusion constant. However, the size of the systematic uncertainty is sufficiently small as compared to the structure of the nonmonotonic dependence of $\rho_{xx}(B)$.

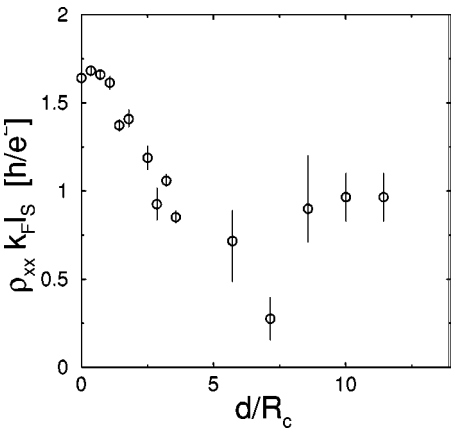

FIG. 12. Magnetoresistivity $\rho_{xx}(B)$ in units of $(h/e^2)/k_F l_S$ (spin included) as a function of d/R_c for a model system specified in the text. Characteristic values of d/R_c are: $R_c/l_S = 1$ at $d/R_c \simeq 0.25$; $\delta/d = 1$ at $d/R_c \simeq 1.8$; $nR_c d = 1$ at $d/R_c \simeq 1.9$; $\pi n R_c^2 = 1$ at $d/R_c \simeq 2.5$; $\delta/2a = 1$ at $d/R_c \simeq 7.1$.

VI. SUMMARY

In summary, we have discussed a rich set of magnetotransport phenomena which take place in a random ensemble of antidots in the presence of long-range fluctuations of a random potential. We believe that the model studied in the paper adequately describes an antidot array in semiconductor heterostructures with a wide spacer for not too high B, when quantum effects (Shubnikov–de Haas oscillations) are still weak. We show that even weak long-range disorder yields a wealth of pronounced effects in the behavior of the magnetoresistance $\rho_{xx}(B)$ in the antidot array. Essentially, these effects are associated with a magnetic-field induced localization of electrons which develops when only one type of disorder is present. As a result of the localization, $\rho_{xx}(B)$ vanishes in the limit of large B both in an idealized antidot system without long-range disorder and in a system with smooth inhomogeneities without antidots. Conceptually, the most striking result of our work is that the interplay of two types of disorder does not simply modify the localization; in fact, it destroys the localization, so that $\rho_{xx}(B)$ even diverges in the limit $B \to \infty$. The divergence takes place despite a strong falloff of $\rho_{xx}(B)$ that occurs in intermediate magnetic fields in the case when one of the types of disorder is sufficiently strong as compared to the other.

Piecing together all the numerous regimes we arrive at a rather complex overall picture, due to the interplay of several distinctly different mechanisms of the MR. Let us list these mechanisms. Some of them are closely related to the mechanisms of the MR characteristic to the limiting cases of strongly non-Gaussian or purely Gaussian disorder. Specifically, we have:

(i) Memory effects operative in the case of strongly non-Gaussian disorder (Lorentz gas, or any other system of rare strong scatterers, without long-range inhomogeneities). These effects lead to a strong *negative* MR (see Sec. II A). In the limit of large B the system is insulating.

(ii) Memory effects in smooth Gaussian disorder. In this case, the memory effects give rise to a strong *positive* MR,

for which, however, the ratio $\rho_{xx}(B)/\rho_0$ cannot be parametrically much larger than 1, since after having reached a maximum value of order 1 it starts to fall off with increasing B, thus yielding a strong *negative* MR (see Sec. II B). In the limit of large B the system is insulating.

In the presence of a long-range random potential, the mechanism (i) of the MR is destroyed by the diffusive motion of electrons scattered by the long-range disorder. Nonetheless, as we have demonstrated in the paper, it is reincarnated in the form of hopping rings (Sec. III C) once the diffusive motion in the long-range disorder turns into the drift with increasing B. In this different form, this kind of a negative contribution to the MR is developed at much larger B as compared to the pure Lorentz-gas system. On the other hand, the mechanism (b) is destroyed by scattering on hard scatterers, which checks the negative MR associated with the adiabaticity of drift in the long-range potential (Sec. III E).

A nontrivial point to notice in our results is that, in addition to the above, there are memory effects that are specific to the inhomogeneous system with two types of disorder. These are:

(iii) ''Diffusion-controlled percolation.'' As we have shown in the paper, scattering by short-range inhomogeneities not just destroys the adiabaticity of motion in a smooth random potential, thus checking the strong negative MR. In fact, it reverses the sign of the MR by giving rise to a *positive* MR which keeps growing with increasing B (Sec. III B). This positive MR is a peculiar feature of percolation of drift trajectories with superimposed diffusive dynamics across the drift lines.

(iv) Renormalization, by long-range disorder, of the collision time for hard scatterers. We have demonstrated that in a system where the hard scatterers give the main contribution to the scattering rate at zero B, a weak smooth disorder can drastically suppress the scattering rate with increasing B (Sec. IV A). The effect takes place for any type of dynamics of scattering by the long-range potential, both for diffusion and drift. The increase of the collision time translates into the *negative* MR.

The overall behavior of the MR is illustrated in Fig. 13. Different curves correspond to different n for given l_S, l_L, and d. The characteristic field B_{ad} marks the diffusion-drift crossover. Figure 13 describes the case of not too weak long-range disorder; specifically, it is assumed that $R_c/l_S \ll 1$ at $B \sim B_{ad}$, which means $l_L/d \ll (l_S/d)^3$.

Having listed the main mechanisms of the MR, let us now summarize our main results. We analyze a ''hydrodynamic model'' of the chaotic antidot array, i.e., tiny antidots scattered with a high density $n \to \infty$ in a smoothly varying random potential (Sec. III B). At large B, $\rho_{xx}(B)$ turns out to be a growing power-law function of the magnetic field. We identified several different regimes of the behavior of $\rho_{xx}(B)$ [Eqs. (14)–(17)], depending on the parameter $l_S/\sqrt{dl_L}$, where l_S and l_L are the mean free paths for scattering on antidots and long-range disorder with a correlation length d, respectively. In the limit $B \to \infty$, the hydrodynamic model universally predicts $\rho_{xx}(B) \propto B^{10/13}$ [Eq. (17)]. The physics of this divergence is a percolation of drifting cyclotron orbits limited by scattering on antidots.

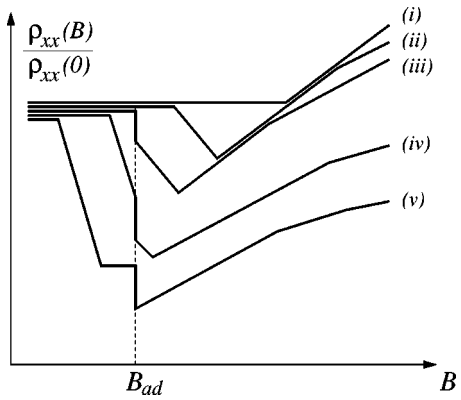

FIG. 13. Schematic behavior of the magnetoresistivity $\rho_{xx}(B)$ on a log-log scale for different values of the concentration of antidots n: $n^{(i)} > n^{(ii)} > \cdots > n^{(v)}$, keeping all other parameters (l_S, l_L, d) fixed. Only one characteristic field B_{ad} is shown, at which the crossover between diffusive dynamics and adiabatic drift in the long-range potential takes place. Different curves illustrate different mechanisms of the magnetoresistance: (i) the magnetoresistance is positive owing to the ''diffusion-controlled percolation;'' (ii) due to the adiabatic localization, the concentration of conducting electrons decreases as $B^{-1}\ln B$ before the percolation becomes effective, which yields a negative magnetoresistance $\rho_{xx}(B) \propto B^{-1}\ln B$ for intermediate B; (iii) an exponentially sharp falloff of $\rho_{xx}(B)$ at $B \sim B_{ad}$ (shown as a vertical jump) separates the diffusive and drift regimes; (iv) because of the memory effects, the collision time for scattering by antidots is increased as compared to the Drude value already in the diffusive regime ($B \ll B_{ad}$), which leads to the negative magnetoresistance $\rho_{xx}(B) \propto B^{-4}$ for small B; (v) for intermediate B, the scattering on antidots stops playing any role and $\rho_{xx}(B)$ is saturated at a value determined by the long-range disorder only, whereas at larger fields the diffusion-controlled percolation gives rise to a positive magnetoresistance.

Relaxing the conditions of the hydrodynamic model, we calculate $\rho_{xx}(B)$ in an antidot array of high but finite density n (Sec. III C). We show that diffusing cyclotron orbits exhibit intricate dynamics by sticking for a long time to a single antidot. This leads to a power-law falloff of $\rho_{xx}(B)$ in an intermediate range of B, namely $\rho_{xx}(B) \propto B^{-1}\ln B$ [Eq. (22)]. The small parameter that governs the physics of this transport regime is $nR_c d$, where R_c is the cyclotron radius. With further increasing B, this mechanism of diffusion is switched off abruptly, in a critical manner [Eq. (23)].

If the long-range disorder is not too weak, we show that the Drude regime and the $B^{-1}\ln B$ falloff are connected via an exponentially fast decrease of $\rho_{xx}(B)$ in a narrow range of the magnetic field, which is a trace of the adiabatic localization in smooth disorder (Sec. III E). In this regime, $\rho_{xx}(B)$ is determined by the interplay of nonadiabatic transitions and scattering on antidots [Eq. (25)].

We calculate the scattering time $\tau_S'(B)$ between collisions with antidots for extended electron trajectories (Sec. IV A), see Eqs. (27), (30), (33), and (38). At large B, τ_S' becomes longer than the Drude time. The smaller n, the earlier τ_S' starts to grow with increasing B. In a very dilute AD array the renormalization of τ_S' starts already in the diffusive regime and leads to a falloff of $\rho_{xx}(B) \propto B^{-4}$ [Eq. (39)].

We solve a scattering problem for a drifting cyclotron orbit colliding with an antidot at small δ/a (Sec. IV B). We study dynamics of cyclotron orbits skipping along the surface of the hard disc and show that the skipping goes on almost adiabatically, which results in a strong suppression of transitions between different drift trajectories [Eq. (53)].

We analyze complex dynamics of skipping cyclotron orbits interacting with an antidot when the ratio R_c/d is large, which includes multiple breakaways from the antidot and multiple returns to it, accompanied by drift along closed trajectories in between (Sec. IV C). We discuss the accumulated effect of these multiple collisions with a single antidot in terms of the scattering shift $R_h(B)$ of the guiding center of the cyclotron orbit after it finally escapes [Eq. (57)]. We also calculate the shift in the limit of a smoothly varying environment [Eq. (55)].

We calculate the percolative magnetoresistance in the antidot array in the limit of small δ/a (Sec. IV D). A variety of different regimes supersede each other with increasing B, all of which are characterized by a power-law behavior of $\rho_{xx}(B)$ [Eqs. (60)–(63)]. The asymptotic behavior of $\rho_{xx}(B)$ in the limit $B\to\infty$ is $\rho_{xx}(B)\propto B^{1/13}$ [Eq. (63)], which from a practical point of view to all intents and purposes is indistinguishable from a saturation of the magnetoresistance. This behavior is in sharp contrast to the localization that would develop in the antidot array in the absence of long-range disorder.

We discuss dynamics of cyclotron orbits which stick to a single antidot for a long time before hopping to another one (similar to the $B^{-1}\ln B$ regime in Sec. III C) in the case of a very weak long-range disorder (Sec. IV E). Taking this limit eventually restores the B^{-1} behavior of $\rho_{xx}(B)$ characteristic to the Lorentz gas.

We present results of numerical simulations (Sec. V). The numerical data qualitatively confirm the predictions of the theory.

ACKNOWLEDGMENTS

We thank M. Heiblum, J. Smet, and V. Umansky for stimulating discussions. We are grateful to D. Weiss for attracting our attention to Ref. 12. This work was supported by SFB 195 and the Schwerpunktprogramm ''Quanten-Hall-Systeme'' of the Deutsche Forschungsgemeinschaft, by INTAS Grant Nos. 97-1342 and 99-1705, and by the German-Israeli Foundation.

*Also at A.F. Ioffe Physico-Technical Institute, 194021 St. Petersburg, Russia.

†Also at Petersburg Nuclear Physics Institute, 188350 St. Petersburg, Russia.

[1] D.K. Ferry and S.M. Goodnick, *Transport in Nanostructures* (Cambridge University, Cambridge, United Kingdom, 1997).

[2] C.W.J. Beenakker and H. van Houten, in *Solid State Physics*, edited by H. Ehrenreich and D. Turnbull (Academic, San Diego, 1991), Vol. 44.

[3] J. Wilke, A.D. Mirlin, D.G. Polyakov, F. Evers, and P. Wölfle, Phys. Rev. B **61**, 13 774 (2000).

[4] A.D. Mirlin, J. Wilke, F. Evers, D.G. Polyakov, and P. Wölfle, Phys. Rev. Lett. **83**, 2801 (1999).

[5] F. Evers, A.D. Mirlin, D.G. Polyakov, and P. Wölfle, Phys. Rev. B **60**, 8951 (1999).

[6] O. Yevtushenko, G. Lütjering, D. Weiss, and K. Richter, Phys. Rev. Lett. **84**, 542 (2000).

[7] S. Cinà, D.D. Arnone, H.P. Hughes, C.L. Foden, D.M. Whittaker, M. Pepper, and D.A. Ritchie, Phys. Rev. B **60**, 7780 (1999).

[8] J. Eroms, M. Zitzlsperger, D. Weiss, J.H. Smet, C. Albrecht, R. Fleischmann, M. Behet, J. de Boeck, and G. Borghs, Phys. Rev. B **59**, R7829 (1999).

[9] G. Nachtwei, Z.H. Liu, G. Lütjering, R.R. Gerhardts, D. Weiss, K. von Klitzing, and K. Eberl, Phys. Rev. B **57**, 9937 (1998).

[10] M. Hochgräfe, R. Krahne, Ch. Heyn, and D. Heitmann, Phys. Rev. B **60**, 10 680 (1999).

[11] I.V. Kukushkin, D. Weiss, G. Lütjering, R. Bergmann, H. Schweizer, K. von Klitzing, K. Eberl, P. Rotter, M. Suhrke, and U. Rössler, Phys. Rev. Lett. **79**, 1722 (1997).

[12] G. Lütjering, Ph.D. thesis, MPI Stuttgart, 1996.

[13] D. Weiss, G. Lütjering, and K. Richter, Chaos, Solitons Fractals **8**, 1337 (1997).

[14] R. Fleischmann, T. Geisel, R. Ketzmerick, and G. Petschel, Physica D **86**, 171 (1995).

[15] D. Weiss, M.L. Roukes, A. Menschig, P. Grambow, K. von Klitzing, and G. Weimann, Phys. Rev. Lett. **66**, 2790 (1991).

[16] R. Schuster, K. Ensslin, J.P. Kotthaus, M. Holland, and C. Stanley, Phys. Rev. B **47**, 6843 (1993).

[17] W. Kang, H.L. Stormer, L.N. Pfeiffer, K.W. Baldwin, and K.W. West, Phys. Rev. Lett. **71**, 3850 (1993).

[18] J.H. Smet, D. Weiss, K. von Klitzing, P.T. Coleridge, Z.W. Wasilevski, R. Bergmann, H. Schweizer, and A. Scherer, Phys. Rev. B **56**, 3598 (1997).

[19] G.M. Gusev, P. Basmaji, Z.D. Kvon, L.V. Litvin, Yu.V. Nastaushev, and A.I. Toropov, J. Phys.: Condens. Matter **6**, 73 (1994).

[20] K. Tsukagoshi, S. Wakayama, K. Oto, S. Takaoka, K. Murase, and K. Gamo, Phys. Rev. B **52**, 8344 (1995).

[21] P.T. Coleridge, Phys. Rev. B **44**, 3793 (1991).

[22] T. Saku, Y. Horikoshi, and Y. Tokura, Jpn. J. Appl. Phys., Part 1 **35**, 34 (1996).

[23] V. Umansky, R. de Picciotto, and M. Heiblum, Appl. Phys. Lett. **71**, 683 (1997).

[24] É.M. Baskin, L.I. Magarill, and M.V. Éntin, Zh. Éksp. Teor. Fiz. **75**, 723 (1978) [Sov. Phys. JETP **48**, 365 (1978)]; É.M. Baskin and M.V. Entin, Physica B **249-251**, 805 (1998).

[25] A.V. Bobylev, F.A. Maaø, A. Hansen, and E.H. Hauge, Phys. Rev. Lett. **75**, 197 (1995); J. Stat. Phys. **87**, 1205 (1997).

[26] A. Kuzmany and H. Spohn, Phys. Rev. E **57**, 5544 (1998).

[27] A. Dmitriev, M. Dyakonov, and R. Jullien, cond-mat/0103490 (unpublished).

[28] D.V. Khveshchenko, Phys. Rev. Lett. **77**, 1817 (1996).

[29] A.D. Mirlin, D.G. Polyakov, and P. Wölfle, Phys. Rev. Lett. **80**, 2429 (1998).

[30] M.M. Fogler, A.Yu. Dobin, V.I. Perel, and B.I. Shklovskii, Phys. Rev. B **56**, 6823 (1997).

[31] M.B. Isichenko, Rev. Mod. Phys. **64**, 961 (1992).

[32] S. Simon and B.I. Halperin, Phys. Rev. Lett. **73**, 3278 (1994).

[33] D.G. Polyakov and B.I. Shklovskii, Phys. Rev. Lett. **74**, 150 (1995).
[34] F. Evers, A.D. Mirlin, D.G. Polyakov, and P. Wölfle, Phys. Rev. B **58**, 15 321 (1999).
[35] B.I. Shklovskii and A.L. Efros, *Electronic Properties of Doped Semiconductors* (Springer, Berlin, 1984).
[36] A.D. Mirlin, D.G. Polyakov, F. Evers, and P. Wölfle, Phys. Rev. Lett. **87**, 126805 (2001).
[37] N. Berglund, A. Hansen, E.H. Hauge, and J. Piasecki, Phys. Rev. Lett. **77**, 2149 (1996).